Title

EXTERNAL MUON IDENTIFIER DEVELOPMENT: HALF METER PROPORTIONAL CHAMBER TEST RESULTS

Author

Parker, Sherwood

Publication Date

1972-05-01

LBL-797
(UH-511-122-72)
(NAL DOCUMENT TM 359)

EXTERNAL MUON IDENTIFIER DEVELOPMENT: HALF METER PROPORTIONAL CHAMBER TEST RESULTS

Sherwood Parker and Ronald Jones

May 1972

AEC Contract No. W-7405-eng-48

LBL-797

DISCLAIMER

LBL-797
UH-511-122-72
NAL DOCUMENT TM 359

EXTERNAL MUON IDENTIFIER DEVELOPMENT: HALF METER PROPORTIONAL CHAMBER TEST RESULTS*†

Sherwood Parker‡
University of Hawaii, Honolulu, Hawaii 96822

and

Ronald Jones
Lawrence Berkeley Laboratory, University of California
Berkeley, California 94720

May 1972

ABSTRACT

A half scale multi-wire proportional chamber has been built to determine the optimum gap and to test several proposed features of the 1 meter chambers that will form the elements of the NAL 15' bubble chamber external muon identifier. The chambers and their readout system are designed to be simple and inexpensive, with machining minimized in the construction. The main features are:

(1) Three coordinate readout--X, Y and U (diagonal), using only one wire plane;

(2) A copper strip--plastic laminate that serves as a gas barrier, cathode, and conveyer of induced signals for the Y and U coordinates;

(3) An electromagnetic delay line readout that also provides a prompt timing pulse; and

(4) A wire-to-wire separation (5mm) sufficiently large to prevent electrostatic instability without the need for supporting structures.

---

*Research supported by U. S. Atomic Energy Commission.

†To be part of a later publication in a technical journal.

‡Address for mail: Lawrence Berkeley Laboratory, University of California, Berkeley, Ca 94720.

A. Introduction

A half scale multi-wire proportional chamber has been built to determine the optimum gap and to test several proposed features of the 1 meter chambers that will form the muon-identifier detector elements. The chambers and their readout system are designed to be simple and inexpensive. The main features are:

1. Three coordinate readout--X, Y (90°), and U (63° now, to be 45° in the 1 m chambers)--using only one wire plane.

2. A copper strip--plastic laminate that serves as a gas barrier, cathode, and conveyor of induced signals for the Y and U coordinates.

3. An electromagnetic delay line readout[1] that also provides a prompt timing pulse.

4. A wire-to-wire separation (5 mm) sufficiently large to prevent electrostatic instability[2] without the need for supporting structures. The system resolution will be limited, in any event, by the delay line electronics cycle time. In principle, however, resolution in the direction parallel to the wire plane can be made much finer than the wire spacing.[1]

5. The 1/2 m chamber gap was made adjustable through the use of spacer frames.

6. The 1m chamber has been designed to minimize machining. Only sawing, drilling, gluing, and soldering will be needed in its construction.

7. The cathode planes are kept flat with a light-weight, non-conducting sandwich material. The 1/2 chamber uses Mylar bonded to polyurethane foam, while the 1m chamber will use Mylar bonded to a paper honeycomb material.

B. The Main Test Results are:

1. A plastic-copper laminate with the copper etched to make conductive strips makes a satisfactory cathode and gas barrier. No charging or shielding problems were observed. A number of subtle

effects were found which played a significant role in the 1 m chamber design.

2. The maximum gain for various gases and gaps was determined. We understand in general, what sets the limits. This information was used in determining the optimum gap thickness.

3. Satisfactory delay line and prompt outputs have been achieved. RMS resolution should be of the order of ± several mm. (The electronics cycle time of 40 ns will broaden this somewhat.)

4. The amplified output from the delay line will easily drive a cable long enough to make the run between Neutrino Labs B and A, eliminating the need for a trailer, electronic racks in a high magnetic field, expensive 66 twisted-pair cable (more $/ft. than coax), and many cold walks in the Illinois snow. We will also be able to monitor the raw signals directly. Tests for electromagnetic interference on site however, remain to be performed.

5. The chamber gave no spurious signals when subjected to a vibration test (hit the table with a hammer). Legitimate signals also did not change in pulse height.

6. The efficiency for perpendicular, charged tracks was measured to be $100 \pm 1/2\%$.

7. The two-pulse resolution depends on the relative size of the pulses and ranges, typically, from 2.5 to 6.5 cm.

8. The following 1/2 m chamber work remains to be done:

   a. Test the chamber in a high magnetic field.

   b. Complete a life test (partly done already with the many hours of running with hot ^{90}Sr, ^{55}Fe, and ^{109}Cd sources).

C. Details and Additional Results:

1. Construction

Figure 1 shows one of the cathode planes. A 1/2 m delay line is shown on the coupling pad region. Figure 2 shows the assembled 1/2 m chamber with the delay lines, preamplifiers, and fiducial driver. Figures 3 to 6 show the 1 m chamber design. The basic idea is to avoid machining by building the chamber of strips sawed from uniform (±0.05 mm), preground sheet of G10 fiberglass which is readily available for not too much more than the basic material cost. One meter strips are sawed with a carborundum table saw in about 30 sec. The finish is smooth, the surface is free of visible carbonization, and the width is uniform to ±0.04 mm.

The cathode planes were made from Kapton bonded to 0.035 mm Cu. The Cu was etched and plated with a thin Au coat to provide the proper strip pattern for the Y (90°) and U (63°) planes. The strips were 2 mm wide and spaced on 2.5 mm centers. A large fraction (80%) of the sheet was made conductive to reduce the cathode field and to prevent gain changes due to charging of the dielectric.

The 1 m chamber will have to use Mylar (0.127 mm)--due to our inability to find Kapton--Cu in sufficient widths. The electrical and mechanical properties of Mylar are just about as good as those of Kapton but it tends to melt when you solder to the Cu if you are not fast. However, we have greatly reduced the number of solder joints needed (from 619 for the 0.2 m chambers (described in Ref. 4) with 1 plane readout to 219--hopefully--for the 1 m chamber with 3 plane readout), and we plan to use impulse soldering for what is left.

2. Uniformity of the cathode planes.

With only a tensioned fine wire plane, and that with 5 mm spacing, the stress on the frame was reduced to the point where the Hexcel was no longer needed for frame support. (There was less than 0.02 mm bowing in 0.4 m.) However, when we tried to do without it, we found the cathode (outer) planes bulged out too much, under small to normal gas pressure differences, making the chamber gain highly non-uniform.

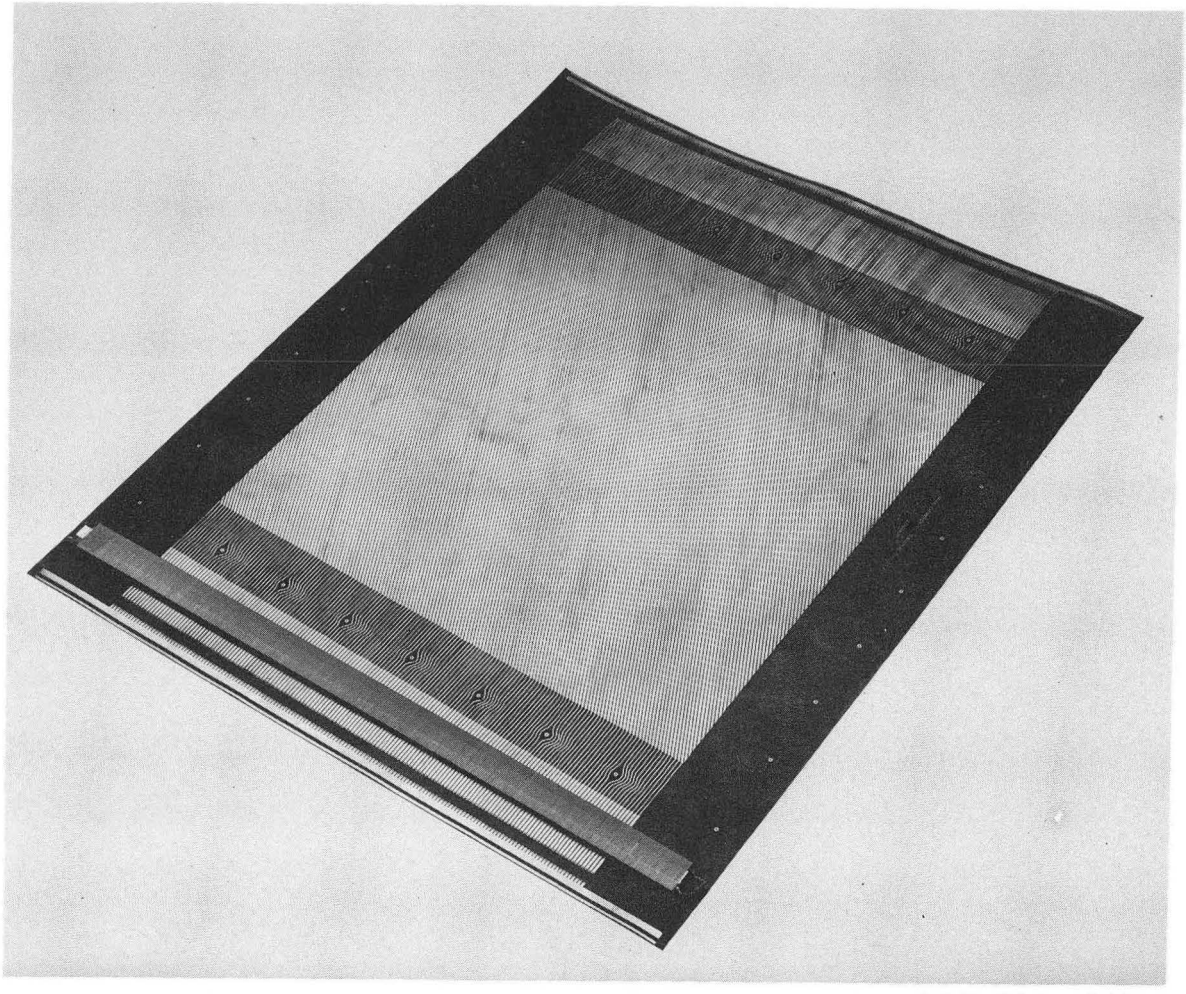

CBB 724-1848

Fig. 1. Cathode plane with a delay line in place.

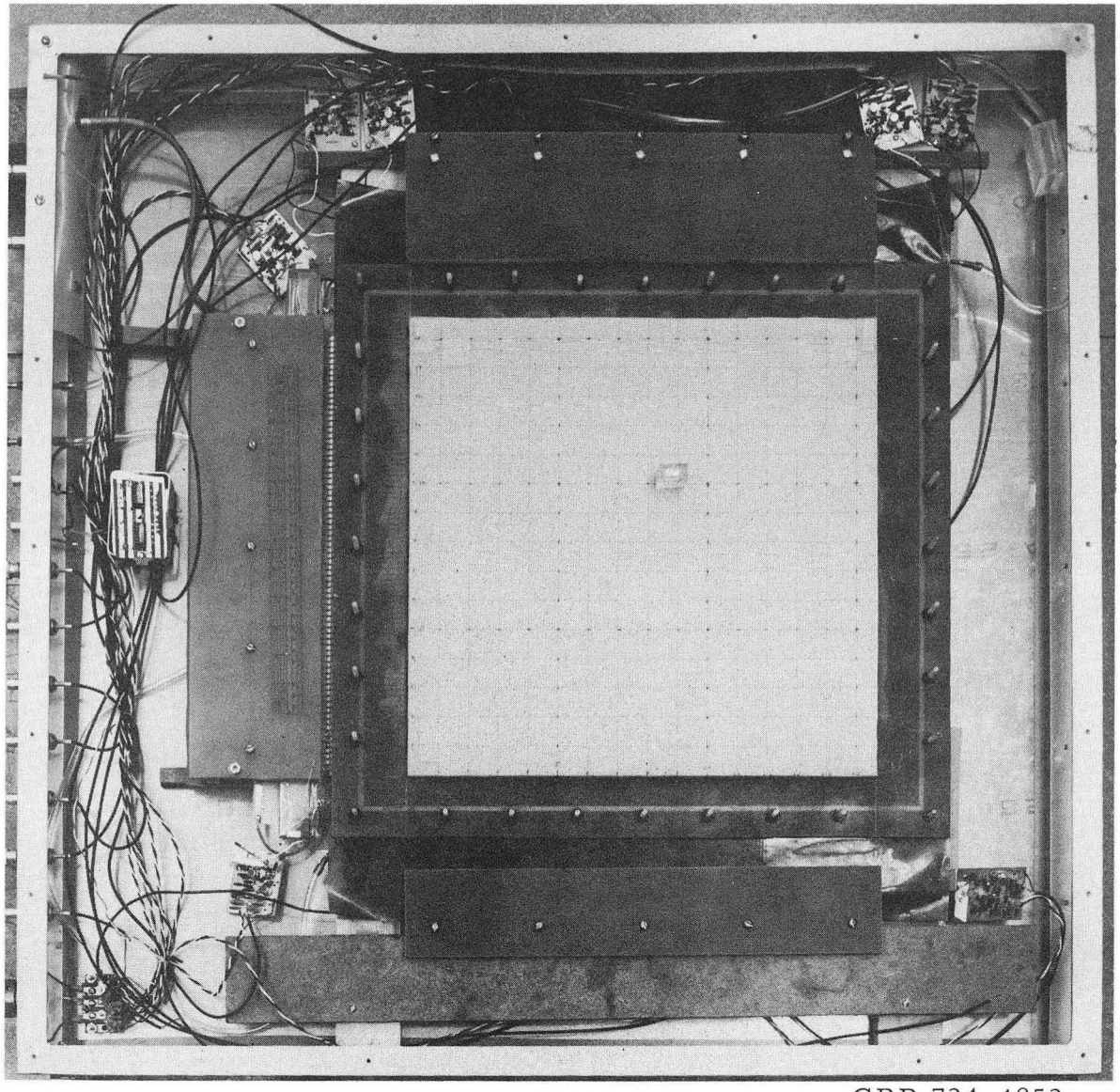

CBB 724-1852

Fig. 2. Assembled 0.5 m chamber with delay line readout.

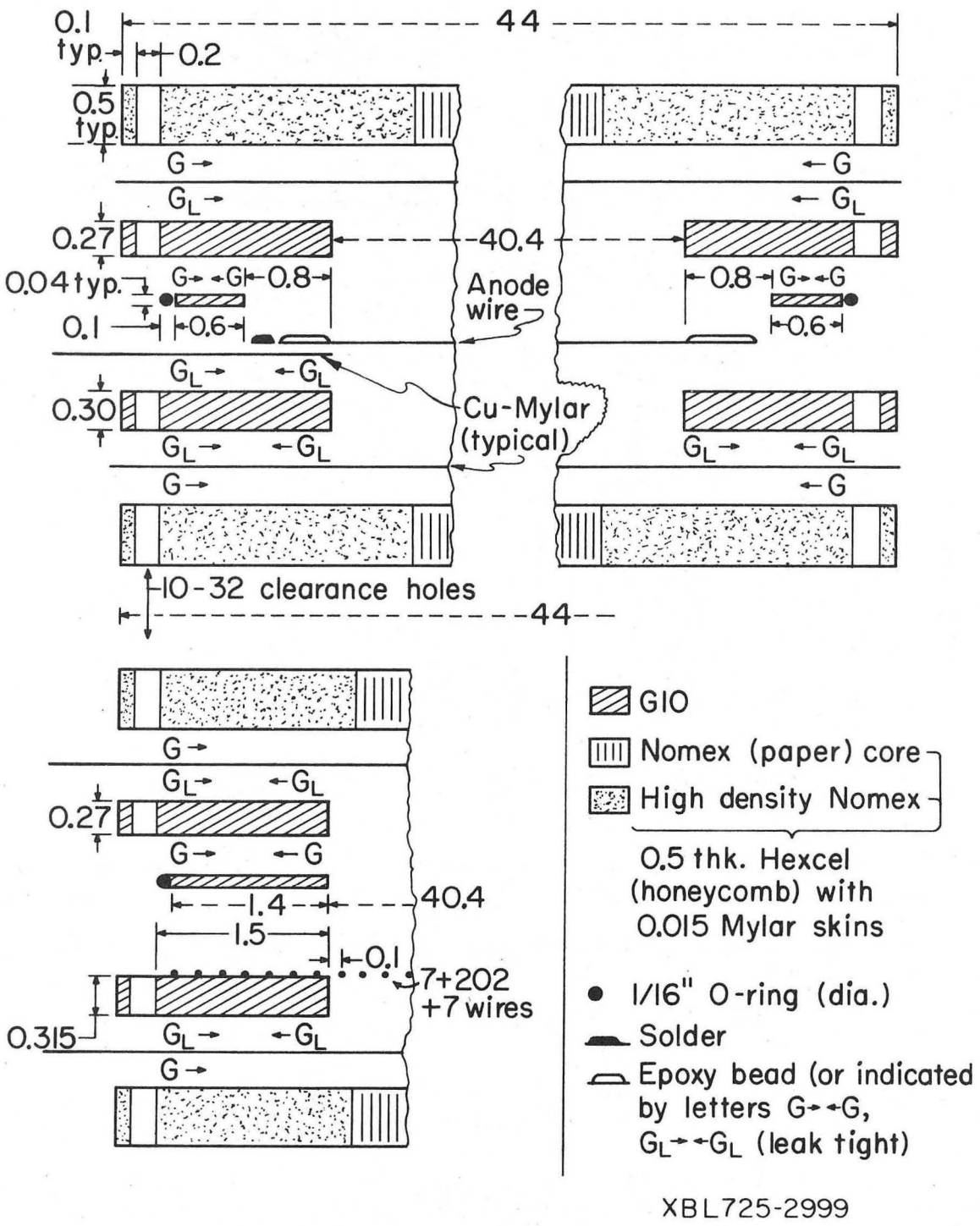

Fig. 3. One meter chamber preliminary sketch-exploded cross-section view. All dimensions are in inches. The wire diameter is 0.0008 in and the spacing is 0.2 in. The G10 fiber glass thickness tolerance is ±0.002 in. The top section is parallel to the anode wires. The bottom shows one side only and is in the perpendicular direction.

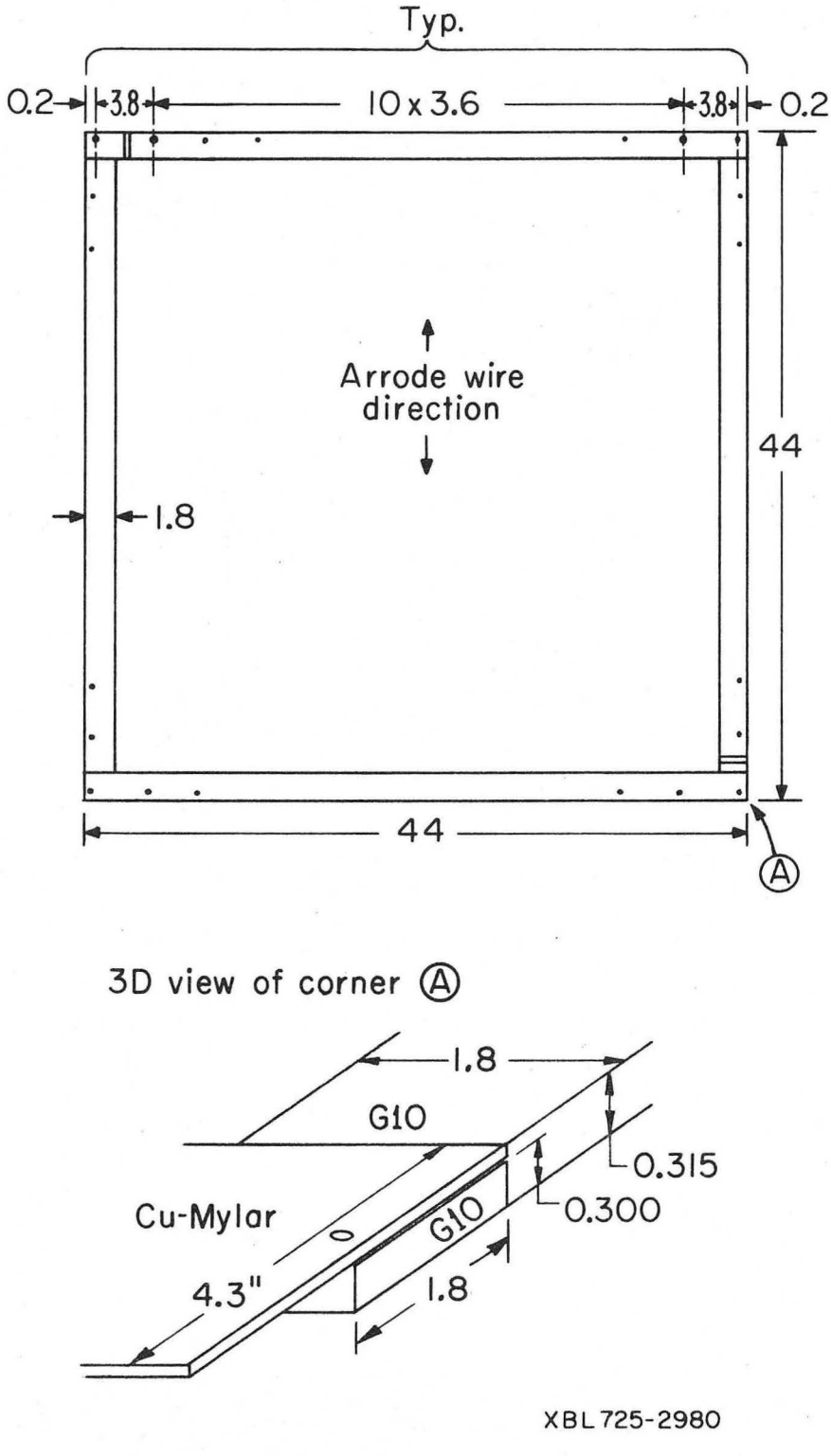

Fig. 4. One meter chamber-bottom G10 frame. The holes are 0.2 inches in diameter. Distances are shown between their centers except the 0.2 in. spacings at the corners are between the center and frame edges.

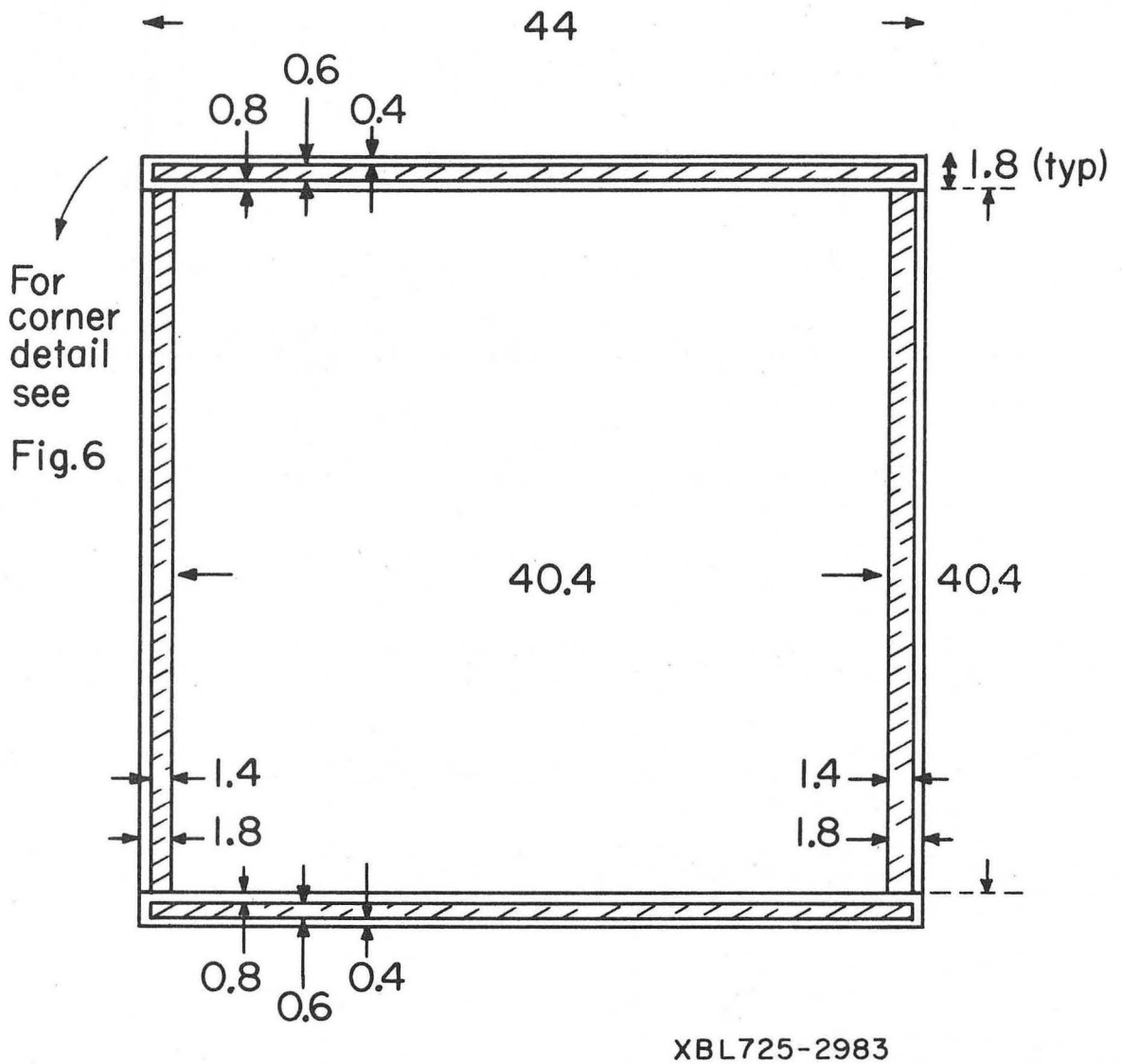

Fig. 5. One meter chamber-top G10 frame (seen from bottom).

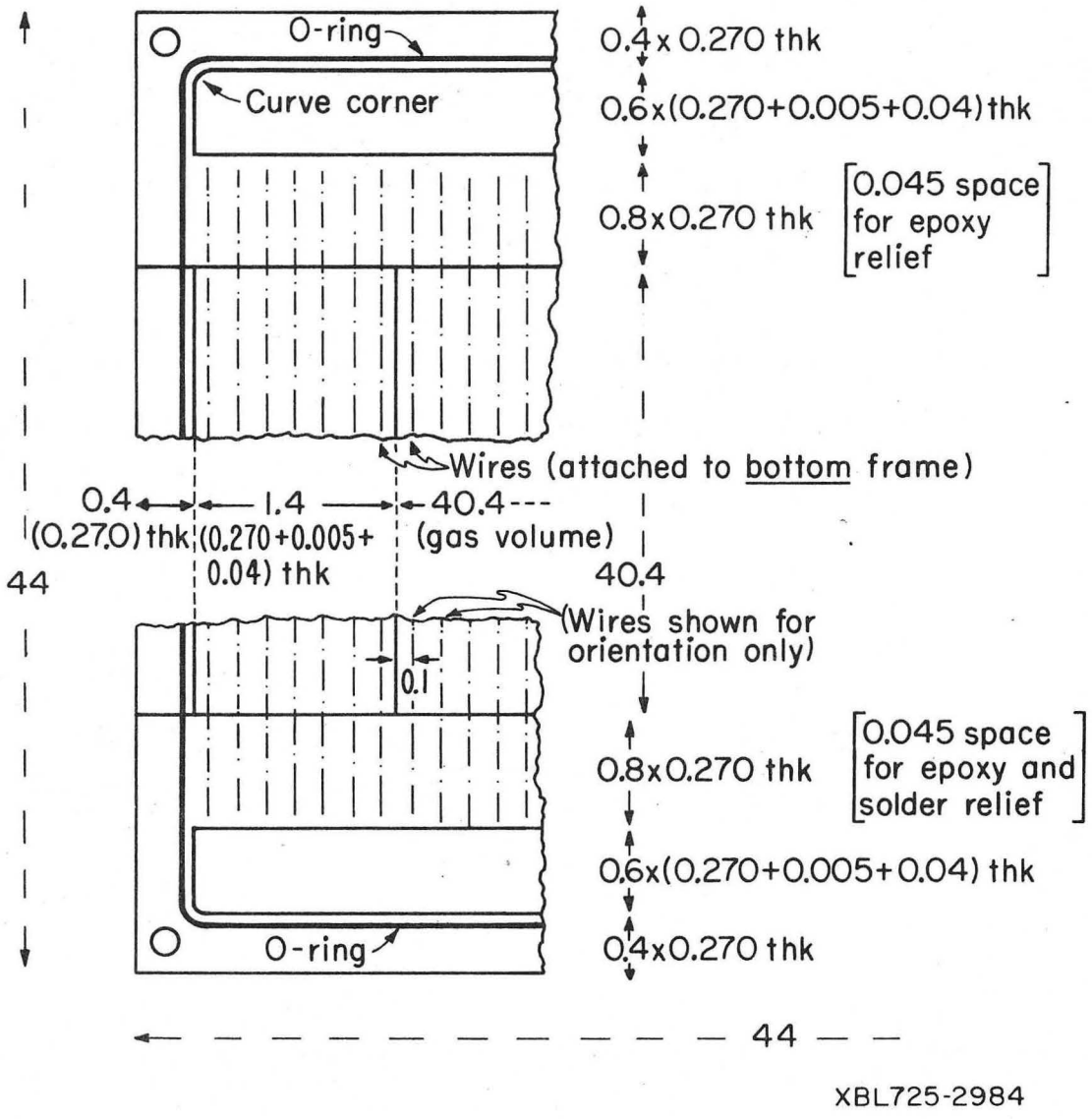

Fig. 6. One meter chamber-corner detail, top G10 frame (seen from bottom).

Supports of 12.7 mm polyurethane foam sandwiched between two 0.38 mm Mylar sheets glued to the Kapton planes made the pulse height uniform to ± 10 to 15% over the entire chamber area to within a millimeter of the edges. When the gap was changed from 2×4 mm to 2×12 mm, signals 2X larger within ~ 1 cm of the edges parallel to the wires and 2X smaller on the other edges were observed. This was due to the cathode plane Cu not continuing over the frame. This edge of the cathode plane printed circuit also caused a small reflection at the point where the delay line crossed it. This reflection (see Fig. 22) can be removed by placing a Cu strip of the proper width under the ends of the delay lines in the present chamber, and by continuing the Cu strips for the delay line length in the 1 m chambers. We confirmed the observation of Ray Fuzesy[3] that thicker outside wires and a wire-free space is not needed for the anode (center) plane, providing the fine wires are laid within the frames on each side (see Fig. 6).

3. Delay line coupling and the cathode planes.

The delay line coupling proved to be much tighter than originally expected (The delay lines were as expected, but we just didn't understand the situation. See section 8 for further details). Two delay lines on the same strips (as occurs for part of the present U plane) consequently load down the signal. To prevent this in the 1 m chamber the strips are at 45° and only go to one of the two U plane delay lines. Along the diagonal, lines of force from avalanches will still split between strips going to both delay lines. Figure 7 shows the signal height as a ^{55}Fe source is moved across the equivalent border in the 0.5 m chamber.

4. The anode plane

The anode plane was wound with 20 μ stainless steel wire.[4] The wire is quite uniform,[5] has its elastic limit at about 75 g and breaks at 100 g. We used a winding tension of 60 g. Figure 8a shows a scanning electron micrograph of the stainless and Fig. 8b shows a similar one of 20 μ gold plated tungsten.

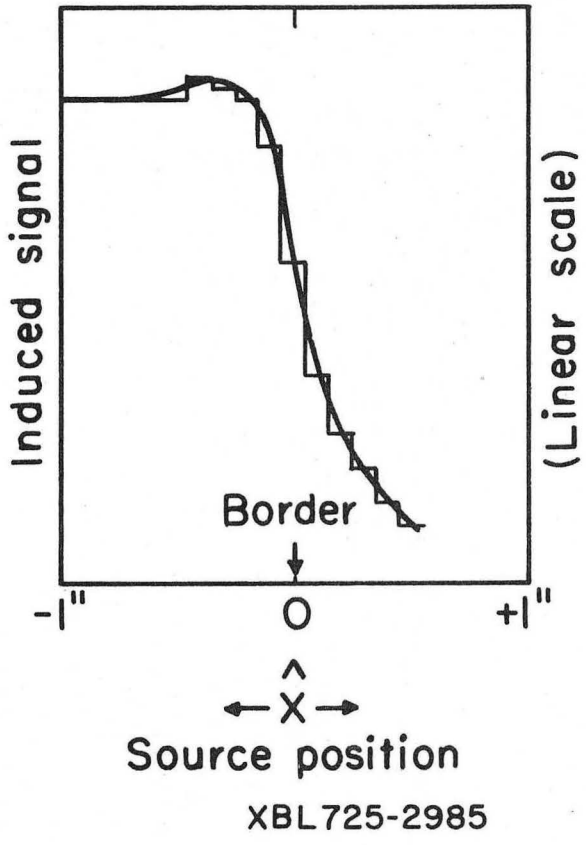

Fig. 7. Induced signal pulse height near dividing border in U cathode plane.

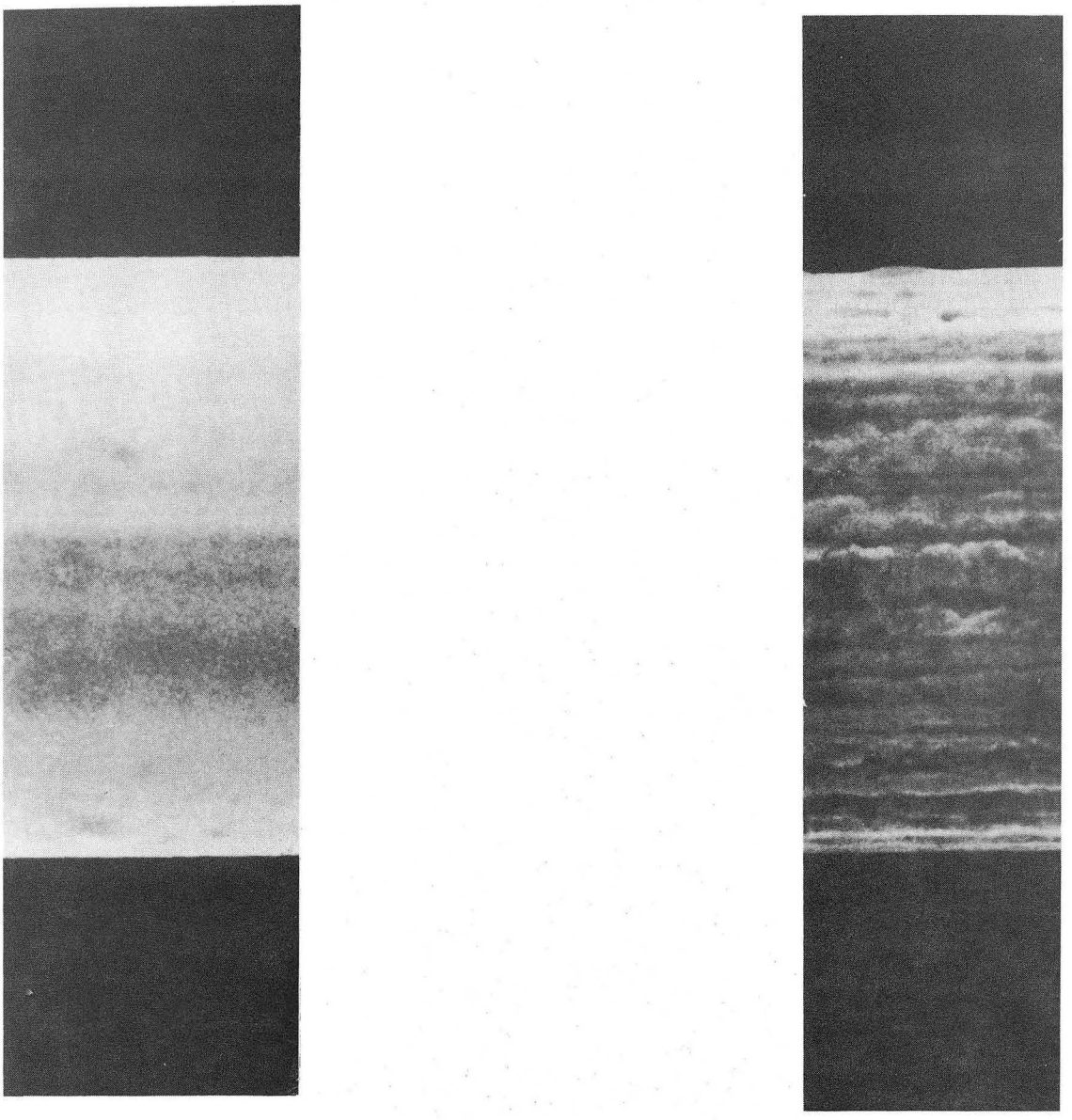

a b

XBB 727-3554

Fig. 8. Scanning electron micrographs of (a) 20 μ stainless steel, (b) 20 μ gold-plated tungsten wire.

The 20 μ plane has proven to be satisfactory. A similar 30 μ one was made but has not yet been tested. To the extent that the adjacent-wire electrostatic instability limits the voltage, a 30 μ plane wound with $(\frac{30}{20})^2$ as much tension would be expected to have a higher ultimate gain (using the gain formula and data from the uniform-gain paper[5] together with Tom Trippe's tension formula). However, that will not limit us. The maximum voltage before the instability sets in is $V \leq \sqrt{T}\ s/C\ell$. Substituting for the capacity, C, of each wire[6], and converting to practical units,

$$V_{(KV)} \leq (980\ T_{(gm)})^{1/2} \left(0.3_{(\frac{V,\,esu}{KV})} \frac{2\pi t + 2s \ln(s/\pi d)}{\ell} \right) \quad (1)$$

where ℓ = wire length, s = separation, d = diameter, and t = half-gap.[2] For ℓ = 1026 mm, s = 5 mm, d = 0.02 mm, t = 8 mm, and T = 60 gm, we get $V \leq 6.67$ kV, well above the expected operating range of 2.5 to 3 kV.

5. The Maximum Gain

The gain proved to be limited by regenerative avalanche feedback. Figure 9 shows ^{55}Fe signals (85% Ar, 15% CO_2, 2×8 mm gap) as the supply voltage is raised. After more than 600 volts change where the only obvious effect is an increase in pulse height, a marked increase in pulse height spread starts at 2720 V. By 2775 there is an increase in pulse duration as well. If the voltage is increased beyond 2800 V, the regenerative processes (ionization by ultra-violet photons and possibly ions that have traveled away from the wire) cause continuous discharges. The increased pulse height spread is presumably also caused by an earlier stage of the same phenomena. Figures 10 to 14 show the pulse height from the anode wire preamp for 2×4, 8, and 12 mm gaps; 5, 10, 15, 20, 25, and 30% CO_2; and ^{55}Fe (5.9 keV x-rays), ^{109}Cd (23 keV x-rays), and ^{90}Sr (2.26 MeV β's passing through 1.27 cm diameter collimators above and below the chamber and triggering a scintillator below it). The delay line coupling was 4.2% and the preamp gain was 430. All ^{55}Fe curves are carried to within 100 V of breakdown. Since we need 100% efficiency, the minimum β pulse height is plotted; pulses of up to three times that are common because of Landau straggling. Despite the factor of two in maximum high voltage as the gap is varied

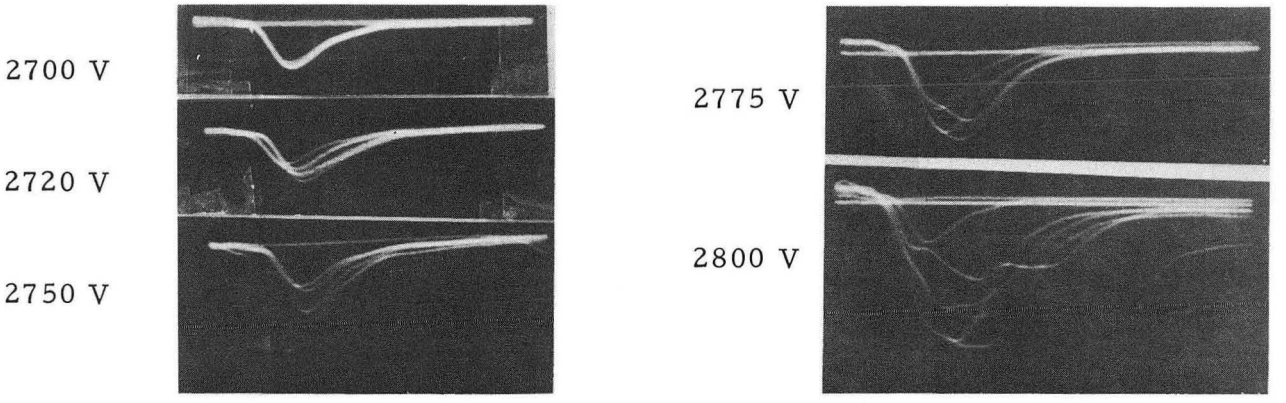

Fig. 9. Wire chamber signals as breakdown is approached. Direct-output (no amplifier) from anode plane delay line, 0.2 μsec/div, 5 mV/div.

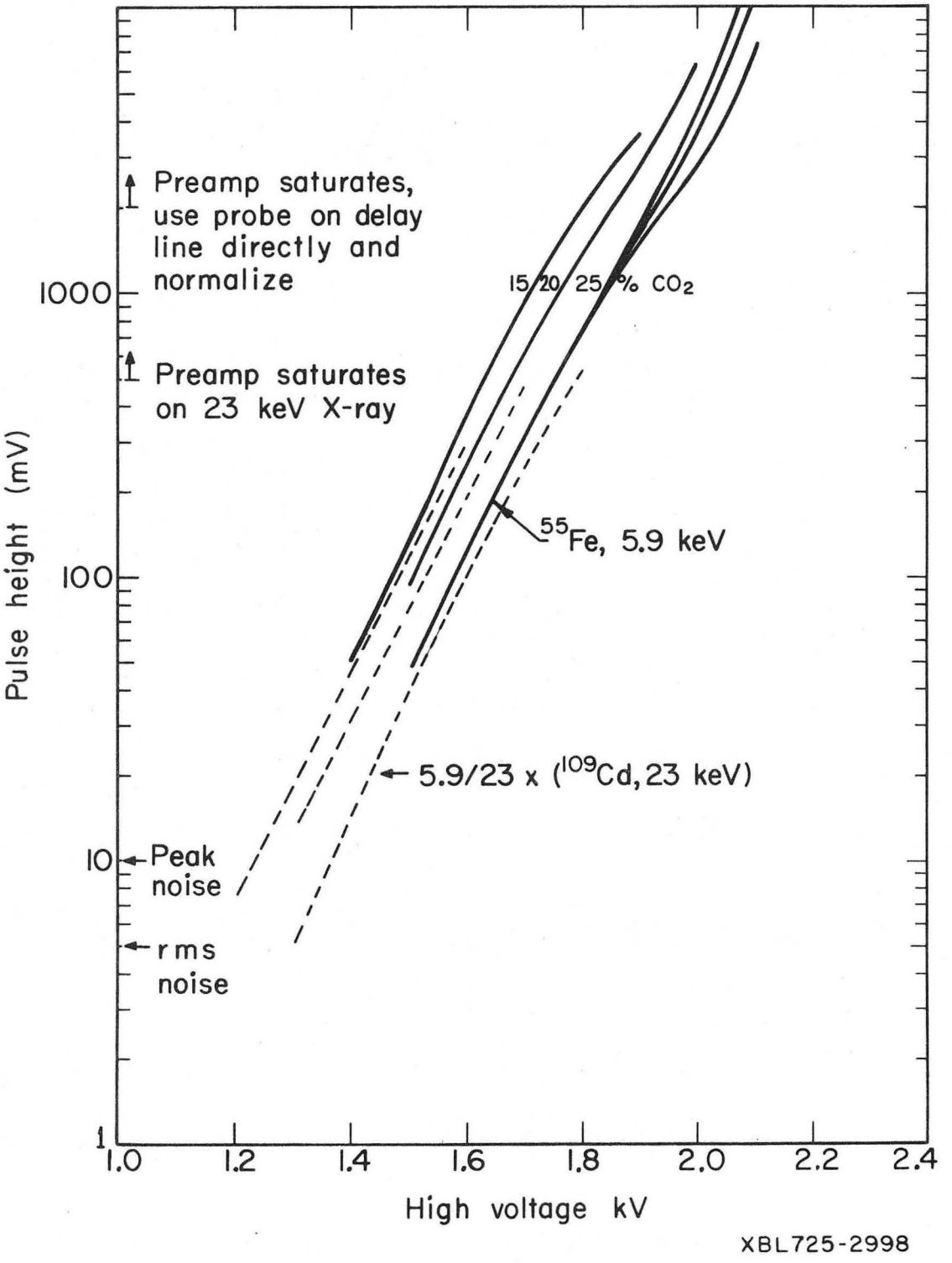

Fig. 10. Wire chamber output vs HV, 2×4 mm gap. Typical pulse height spreading approaching breakdown is shown for the 25% CO_2 curve.

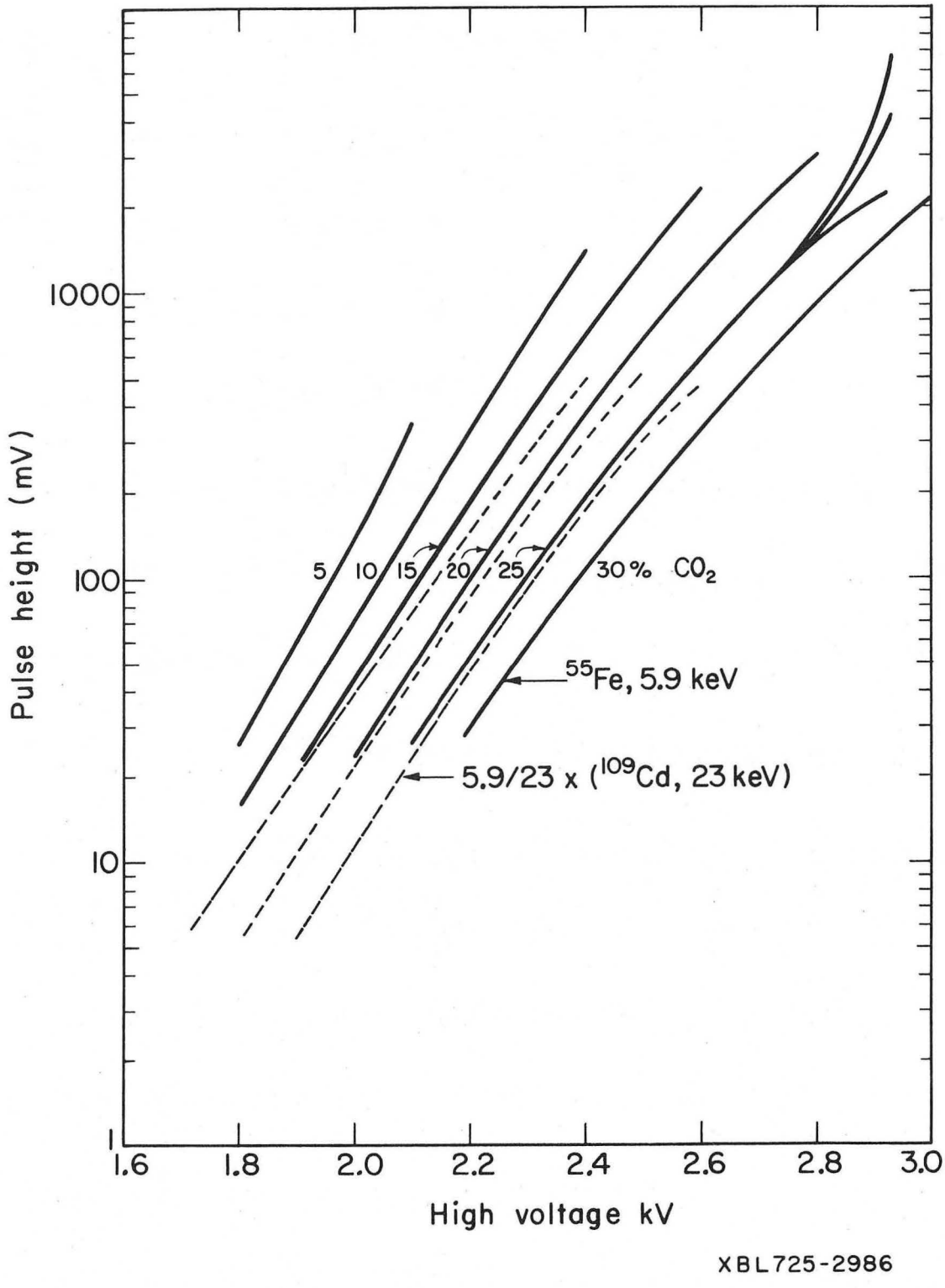

Fig. 11. Wire chamber output vs HV, 2×8 mm gap. Typical pulse height spreading approaching breakdown is shown for the 25% CO_2 curve.

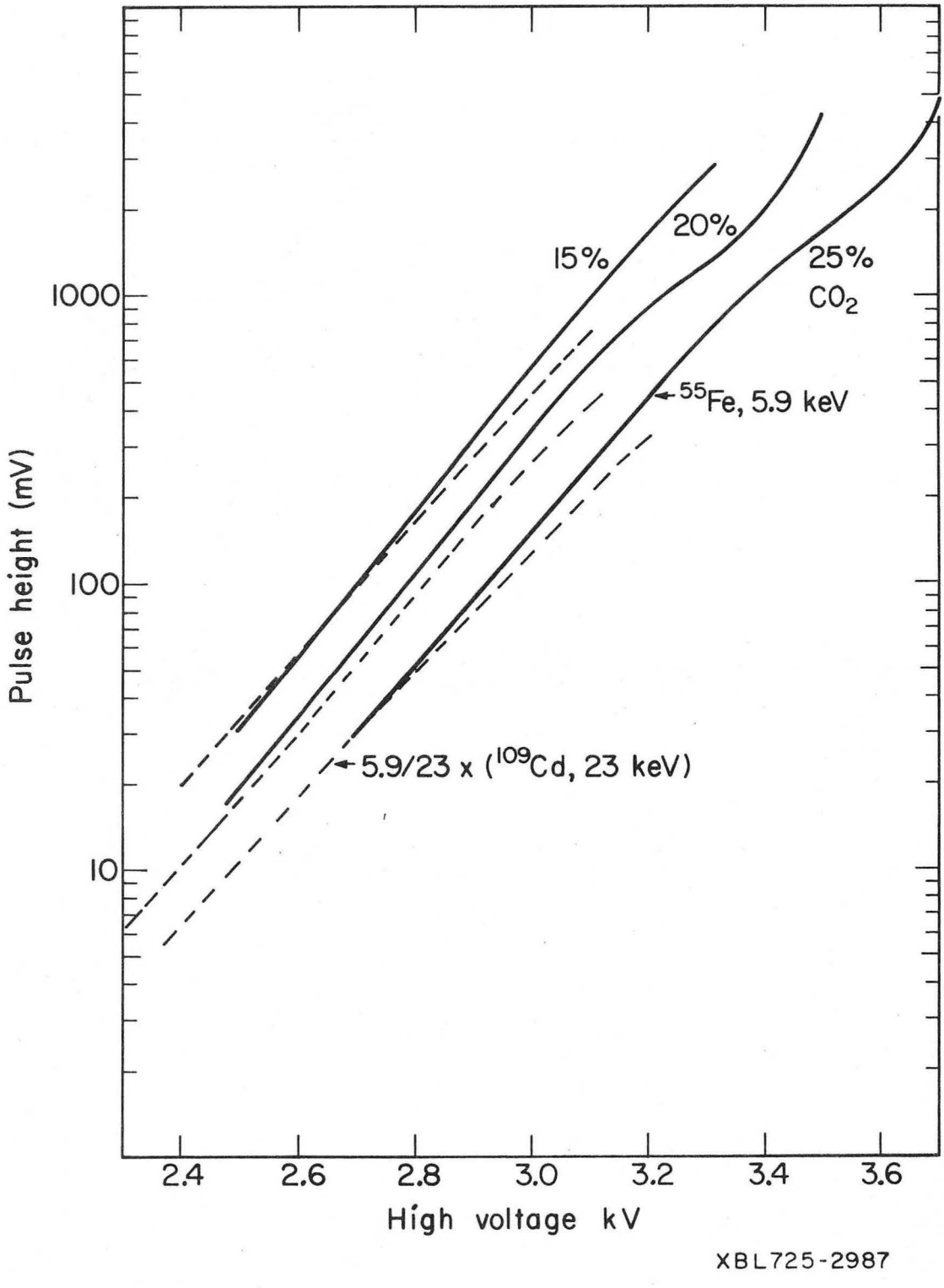

Fig. 12. Wire chamber output vs HV, 2×12 mm gap.

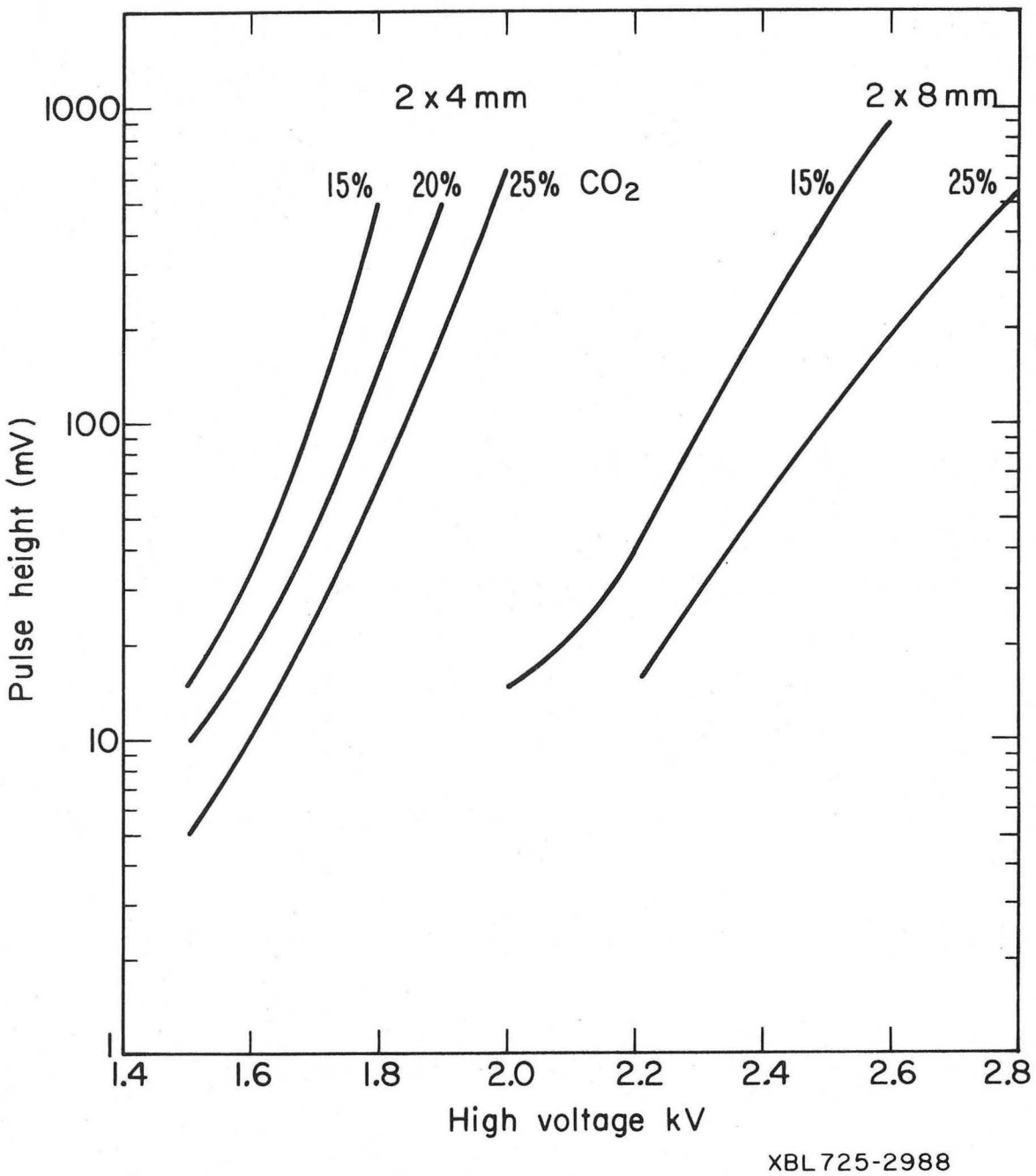

Fig. 13. Wire chamber output-minimum pulse height of ^{90}Sr β signals vs HV for 2×4, 2×8 mm gaps.

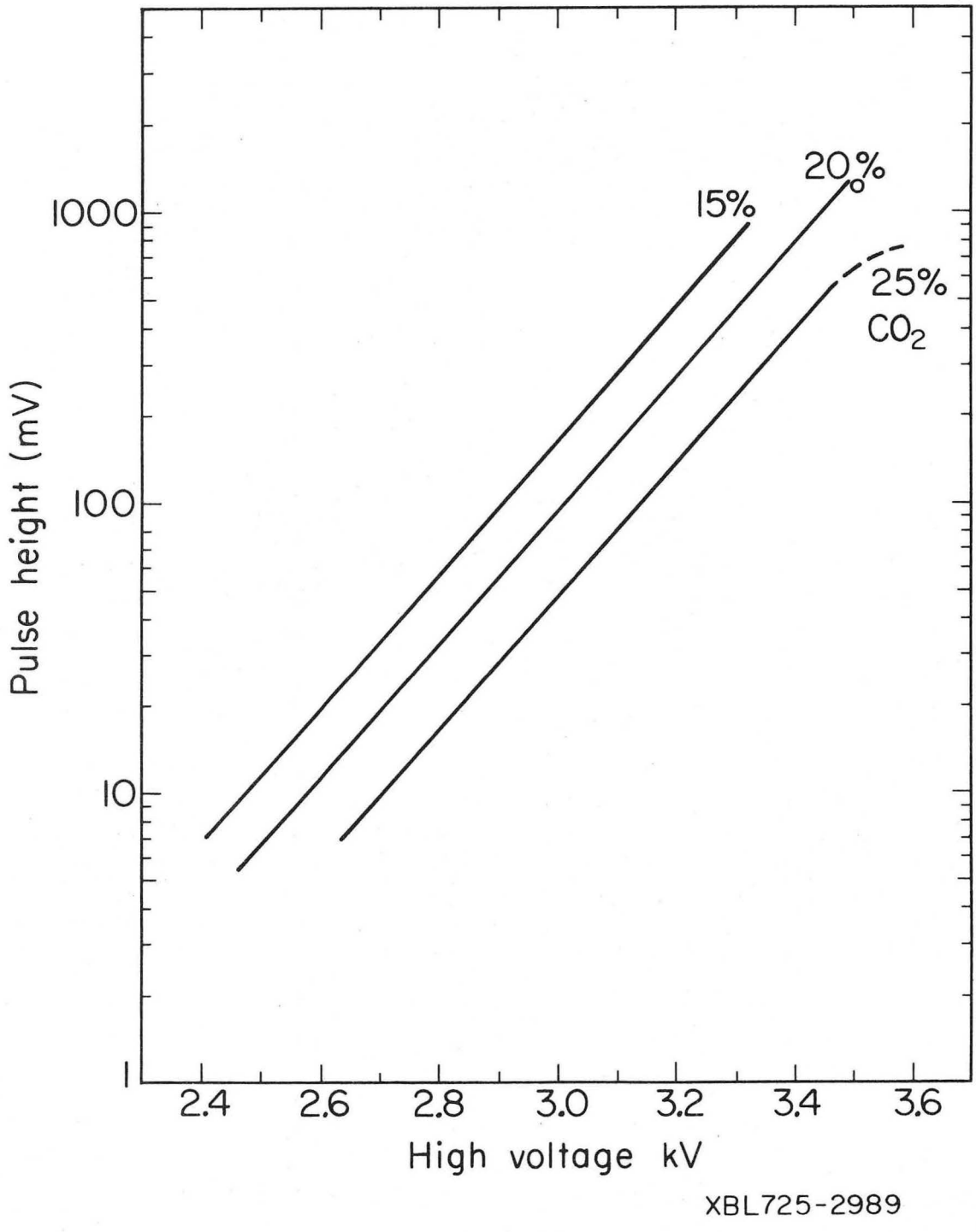

Fig. 14. Wire chamber output-minimum pulse height of ^{90}Sr β signals vs HV for 2×12 mm gap.

from 2×4 to 2×12 mm the maximum attainable pulse height is the same within measurement errors. In all cases the approach to breakdown is qualitatively unchanged from Fig. 9.

When the percentage of CO_2 is increased, the gain drops, presumably from an increase in inelastic, non-ionizing collisions. Consider Fig. 11. An ~ 18% increase in voltage is necessary to restore the gain when the CO_2 is increased from 5% to 25%. Now, however, it is possible to raise the voltage still further and get a larger ultimate gain since an increased fraction of the photons that could start new avalanches are being absorbed in exciting (but not ionizing) CO_2.

Several other features of the curves are of some interest. A comparison of the 23 keV and 5.9 keV x-rays shows proportionality of gain at low values and the onset of space charge saturation at the higher values. This probably also causes the reduction from the exponential voltage dependence of the ^{55}Fe pulse height since the simple theory that predicts a near straight line (see formula (1) and references in the uniform gain paper)[5] allows for neither space charge nor regenerative effects.

The source-off counting rate is voltage independent to within 200 volts of breakdown providing the counting threshold is set at a constant fraction of the ^{55}Fe pulse height. For 10, 50, and 100% of 5.9 keV, it was measured to be 76, 54, and 43 counts/second. These numbers include counts from approximately 27 cosmic rays/second and do depend somewhat on the state of cleanliness of the chamber. Guard strips have never been tried, are presumably unnecessary, and would complicate the construction. Wires finer than 20 μ would probably allow a yet higher maximum gain, so long as the electrostatic-force limit is not exceeded. At one extreme, it is known that a parallel plate, DC proportional chamber cannot be made; it breaks down. On the other, Rich Muller and Steve Derenzo, using 3.6 and 5 μ dia. wire have reached gas gains in pure xenon--no quencher at all--of over 40,000.[7] The best we have done in pure argon with 20 μ wires is 100. Furthermore, we had all sorts of trouble with breakdown in the field intensification region of the gas tubes in our lead-plate spark chambers

when we had large diameter holes. Smaller holes with their necessarily greater intensification, nevertheless, gave no trouble. All this leads one to suspect that minimizing the volume of gas in high fields may be desirable. Someday, after we have experience in winding and operating 20 μ chambers, it might be desirable to try one with 10 to 15 μ wire. No other accompanying changes would be needed, providing the tensioning device could handle this range.

6. Selection of the Gap Thickness

The maximum measured gas gain does not change significantly with gap. However, the track length is proportional to the gap, and since we do not use electro-negative gasses, we collect all the electrons. Also, since the delay lines sum and interpolate to find the center of inclined tracks, the usual multiple signal problem with individual wire readout is not present. Larger gaps, in addition, reduce the sensitivity of the gain to gap non-uniformities. Examination of Figs. 10 to 14 indicates that for a constant output voltage, V_{supply}/t decreases as the half gap, t, is increased. From formula (1) it can be seen that such a decrease makes the tension requirement less stringent.

What finally sets an upper limit to the gap is a completely different phenomena: incoherent addition of the induced pulse at the delay line. As the positive ions pull away from the anode wire, the matching electrons that were held nearby on the wire also leave, following it out to the power supply. The field induced by the now unbalanced positive charge is spread over a length comparable to the gap thickness when it reaches the outer plane. Figure 15 shows the measured spread for 2×8 and 2×12 mm gaps. When this distance becomes comparable to $(v_{\text{delay line}})\times(\tau_{\text{pulse width}})$ the induced signal amplitude decreases. For 2×4, 8, and 12 mm gaps the induced signal was 33, 40, and 15% of the wire plane signal. (Our 0.2 m chamber gave 40%.) The maximum expected is 50%. This can be seen as follows. Suppose n electrons are collected on the central anode wire, p_w positive charges are induced on the adjacent anode wires, and $1/2(n - p_w)$ charges are induced by the remaining lines of force on each of the cathode planes.

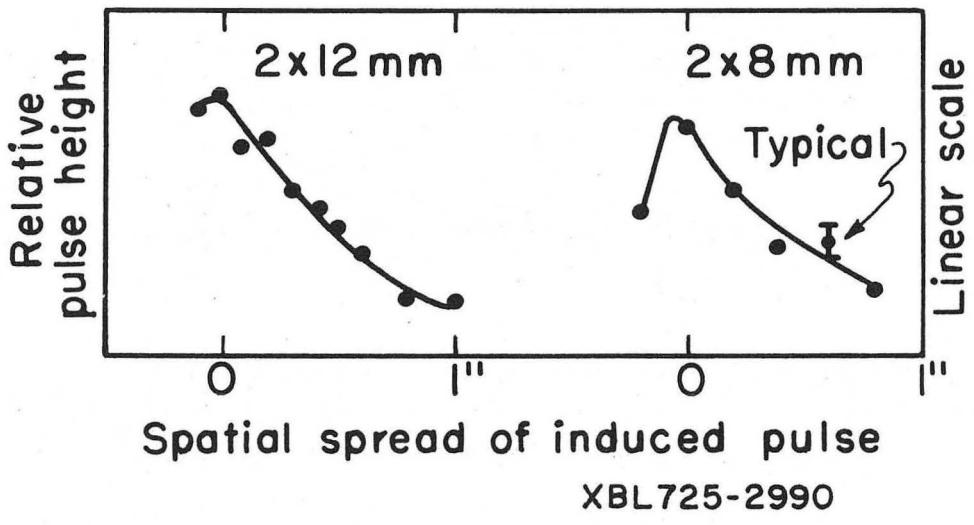

Fig. 15. Spatial spread of induced pulse for ^{55}Fe source at position 0.

Neglecting phase lags in the addition at the delay lines, the ratio [cathode signal]/ [anode signal] will be $[1/2\ (n-p_w)]/[n-p_w]$. The ratio for 2×8 mm, 40% is quite satisfactory. However, the 2×12 mm ratio, combined with the other major sources of pulse height spread, the Landau effect (3:1), delay line attenuation (at least 2:1) and track length variations (say 1.5:1) would present the amplifiers with a required dynamic range of 60:1; possible, but very uncomfortable. One question remains: why is the ratio down to 33% at 2×4 mm. It's not clear. It may be part measurement error, and part reduced coupling at the delay line, since the signal comes in on fewer strips and hence sees a lower capacity to the delay line.

7. Efficiency

The efficiency for all gaps was measured to be 100% with an error of 1/2%, and thus played no role in chamber design. The scope was triggered on ^{90}Sr counts from a scintillator under the chamber. Half-inch lead collimators were used both above and below the chamber. A definite minimum β pulse height was seen (see Fig. 16.) Occasional zero height pulses were also seen at a rate compatible with the phototube noise rate. Two typical runs of equal duration at 2×8 mm gave:

1115 triggers, collimator open - 1102 counts + 13 zero height traces
54 triggers, collimator closed - 38 counts + 16 zero height traces.

8. Delay line performance

The use of flexible circuit boards clamped to the delay lines has produced a reliable coupling. The delay line that is placed on the high voltage plane is wrapped with three turns of 12.7 μ Mylar and kept at ground. (It is much easier to make the transition from high voltage in the high impedance part of the circuit. When the signal is on the ~ 1 kΩ delay line, headed for a ~ 1kΩ termination, any series capacitor must have $1/\omega C \ll 1K\Omega$ and hence a $C \gg 100$ pF. Disc ceramics are rather noisy and glass encased ones in that capacity and

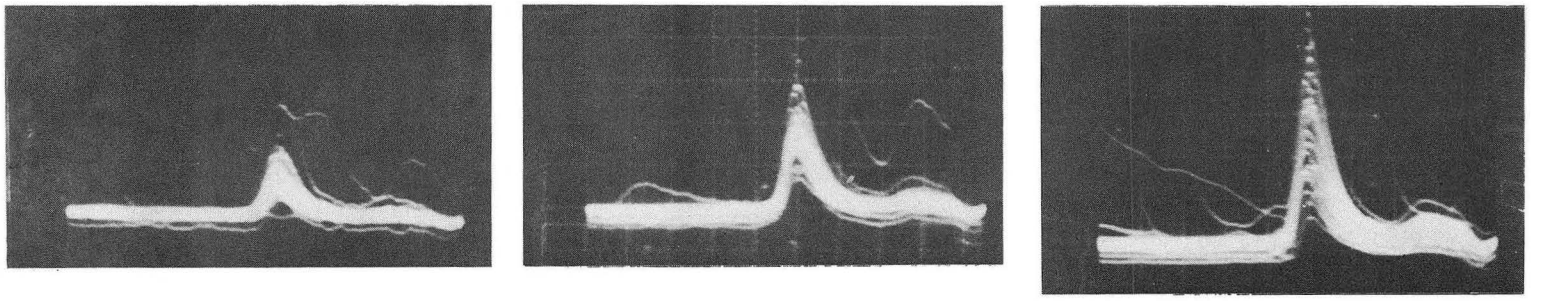

a b c

XBB 727-3556

Fig. 16. β pulses triggered by a scintillator on the far side of the chamber. 2×8 mm gap, 25% CO_2 - 75% Ar, 0.5 μsec/div, 50 traces each, (a) 0.1 V/div, HV = 2.4 kV, (b) 0.2 V/div, HV = 2.6 kV, (c) 0.5 V/div, HV = 2.8 kV.

voltage range are large, expensive, and a general nuisance.)

Figures 17a and b show ^{55}Fe pulses from one end of the wire plane delay line when the scope is triggered by the other end. Due to the quantization of the avalanche positions by the wires, the pulses come out at discrete positions with the only scatter being a ± 0.2 mm spread due to noise. Figure 17c shows similar pulses from the induced plane (Y) delay line for two positions of the source separated by 1 cm. Now a spread about each position of about ± 1.5 mm can be seen. This is reasonable considering the dimensions of the source.

The delay line coupling was measured by taking the ratio

$$\frac{\text{V, 1:1 scope probe at delay line end}}{\text{V, 1:1 probe on printed circuit pad}} = \frac{1.8\ \text{mV}}{11.5\ \text{mV}}.$$

The delay line and preamplifier were in place for both measurements. This figure includes the normal (small) attentuation for the last few inches of the delay line, but does not include a correction for the extra loading of the pad signal by the probe capacity. This is measured by measuring

$$\frac{\text{V, preamp, probe on pad}}{\text{V, preamp, probe off}} = \frac{145\ \text{mV}}{434\ \text{mV}}.$$

The final result is then $(1.8 \times 145)/(11.5 \times 434) = 5.3\%$. A similar measurement with the same delay line wrapped with Mylar for high voltage service gave 4.2%. The original 0.5 m delay lines (6.35 mm $\times$ 19 mm cross section, 19mm wide ground strip, No. 36 wire, 7 nsec/mm) were used for this measurment. Newer lines (4.8 mm $\times$ 25.4 mm cross section, 12.7 mm wide ground strip, No. 38 wire, 7 nsec/mm) have a coupling greater by a factor of 10/9.

Attempts that have been made to increase this figure by doing such things as scraping off the insulation and soldering the delay line wires to the pads would not be expected to have much effect however, (other than wrecking the delay line) because the capacitative coupling to the delay line is already quite tight. This showed up clearly when we tried to take a prompt signal out by looking at the end of the 470 kΩ resistors as shown in Fig. 18. Almost nothing came out! Not until

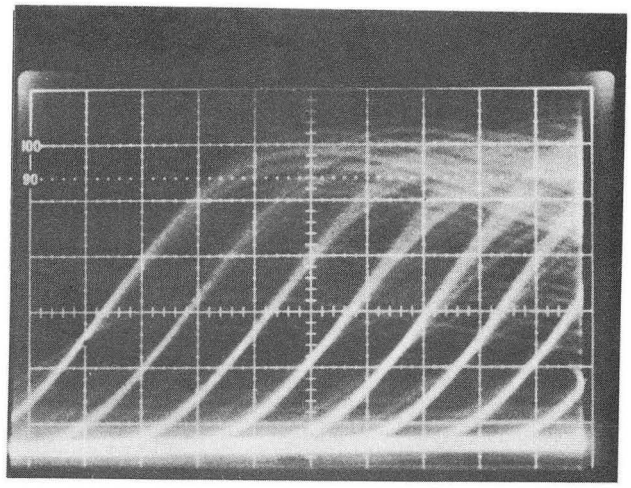

a

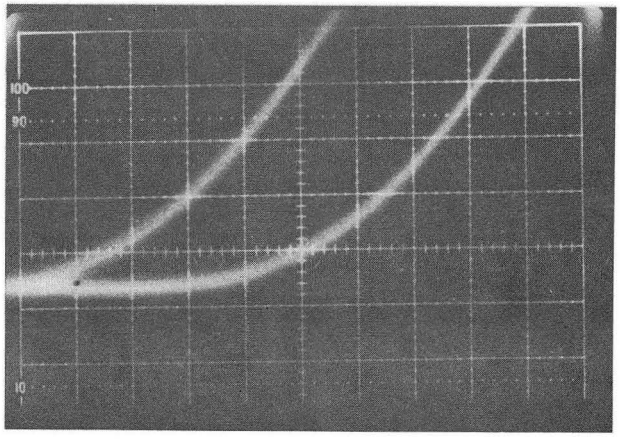

b

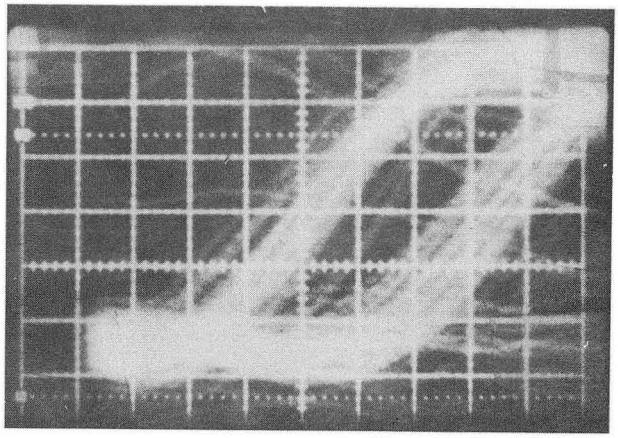

c XBB 727-3557

Fig. 17. Delay line pulses from collimated ^{55}Fe source. 2×4 mm gap, 20% CO_2 - 80% Ar, HV = 1.7 kV. (a) Anode plane, showing position quantization, 200 m V/div, 50 nsec/div, (b) Same, 50 m V/div, 20 nsec/div, (c) Cathode plane, 100 m V/div, 50 nsec/div.

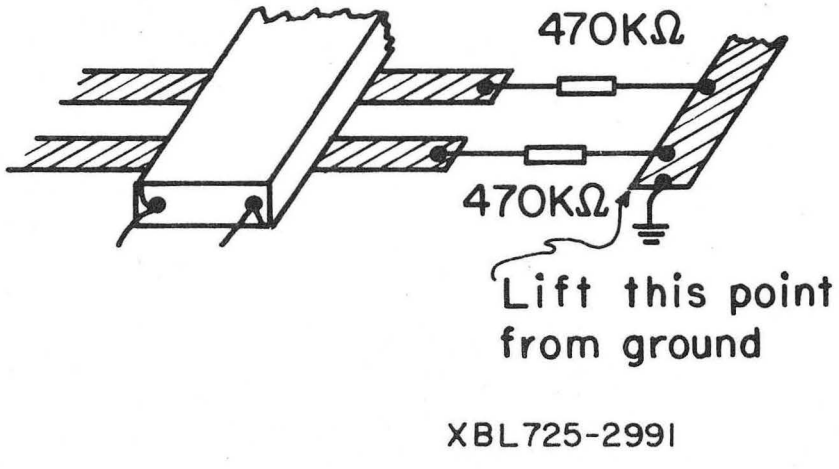

Fig. 18. Delay line and ground plane-prompt signal.

the 470 kΩ was reduced to the point where the delay line signal was being degraded (due to the low, position dependent, shunt impedance of all the parallel resistors), was much signal seen. Most of the current was going into the delay line; when it was lifted from the pad, the signal increased by a factor of 5. This was also seen on the U plane. Those strips that ran to 2 delay lines produced a signal only 1/3 as large (see Fig. 19). This would not happen if the delay line were only loosely coupled to the pad.

The ratio of the delay line voltage to chamber voltage is considerably less than unity largely because the delay line has a relatively low impedance and is being fed by a high impedance current source (the chamber). Positive ions in the chamber move away from the anode wires at a rate determined by the high voltage. As they do, the avalanche electrons that were collected on the wires are released from them, pass through the power supply and go to the cathode plane where they are attracted by the approaching positive ions. The delay line is in series with this circuit (for fast AC signals), so the signal voltage will be ~I(Z/2) where Z, the delay line impedance is only ~ 1 kΩ (currently).

Consider the cross section view of the delay line shown in Figs. 20 and 21a. Electrons released from the anode wire appear on the pad and momentarily change the potential of the delay line windings and ground strip. Positive charges, attracted to the low impedance ground strip, quickly bring its potential back to zero. The windings, isolated by their high inductance, remain at about 70% of the pad potential (as estimated by modeling the configuration with conductive paper). About 95% of the lines of force between the pad and ground strip go by way of the windings as shown in Fig. 21b. The positive surface charge on the windings is held in place by the negative charge on the pad. The negative charge together with the matching positive charge on the ground strip, driven out initially by Coulomb repulsion, forms waves of charge of q/2 moving out in either direction along the delay line as in Fig. 21c. The voltage corresponding to this charge would be half of the initial

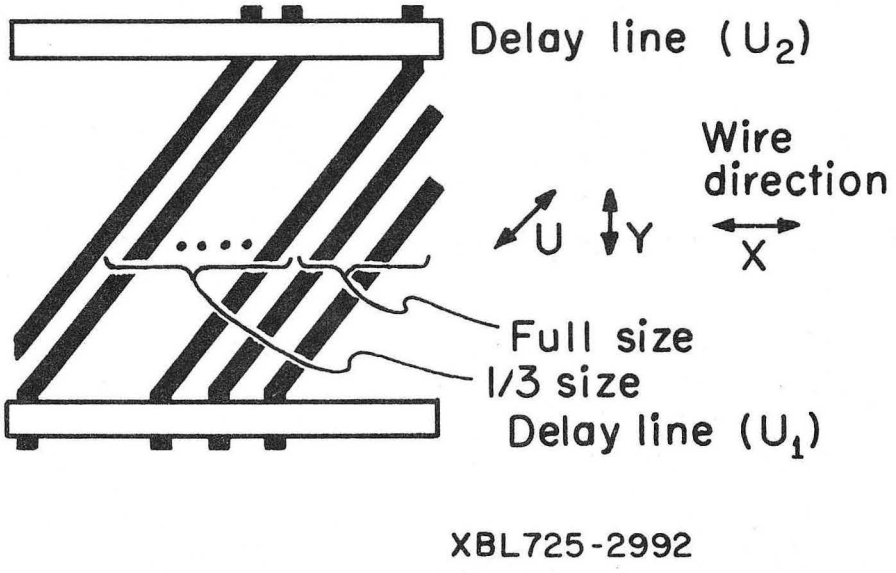

Fig. 19. Delay lines on U plane.

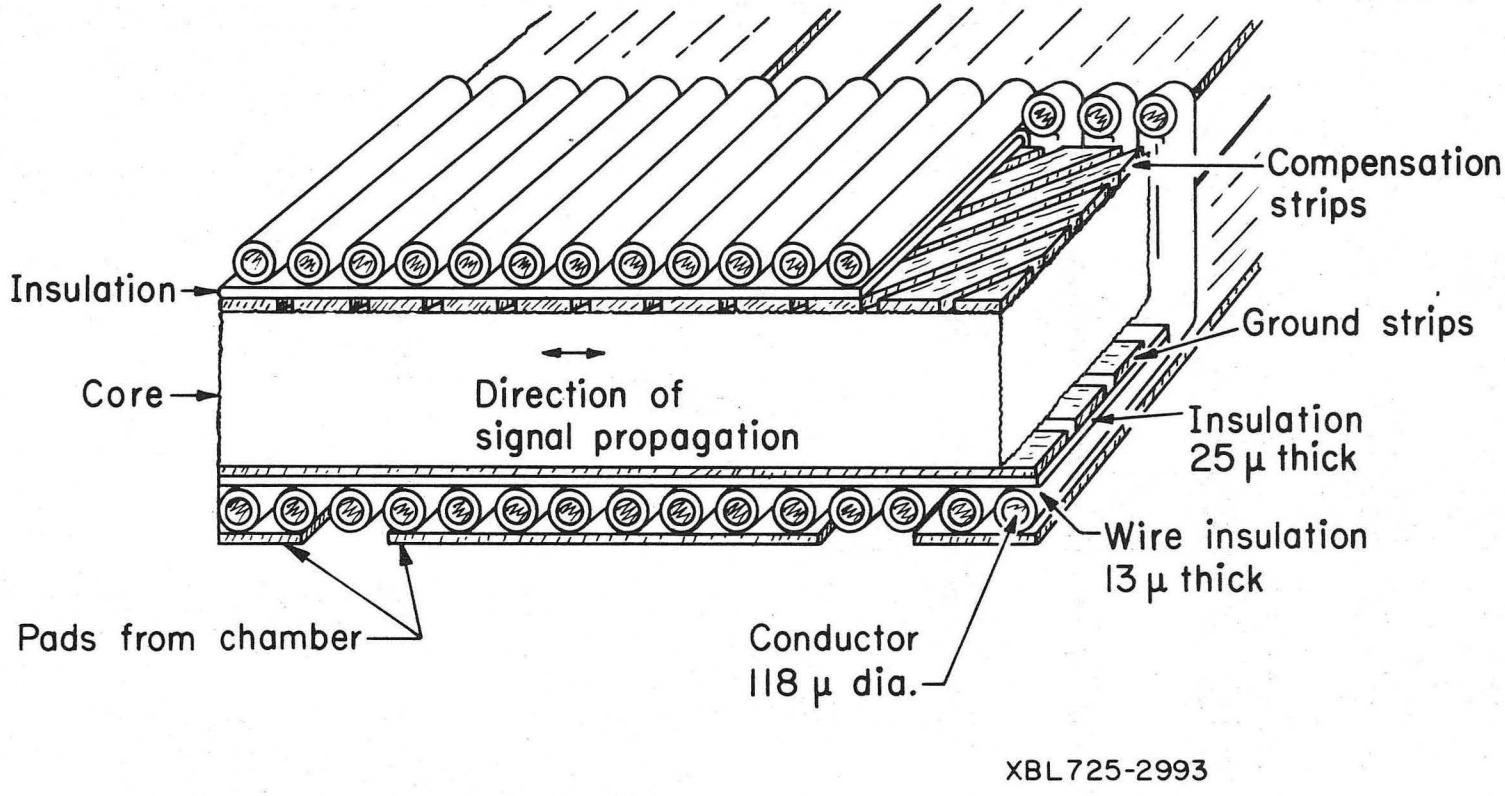

Fig. 20. Cross section view of delay lines and chamber pads.

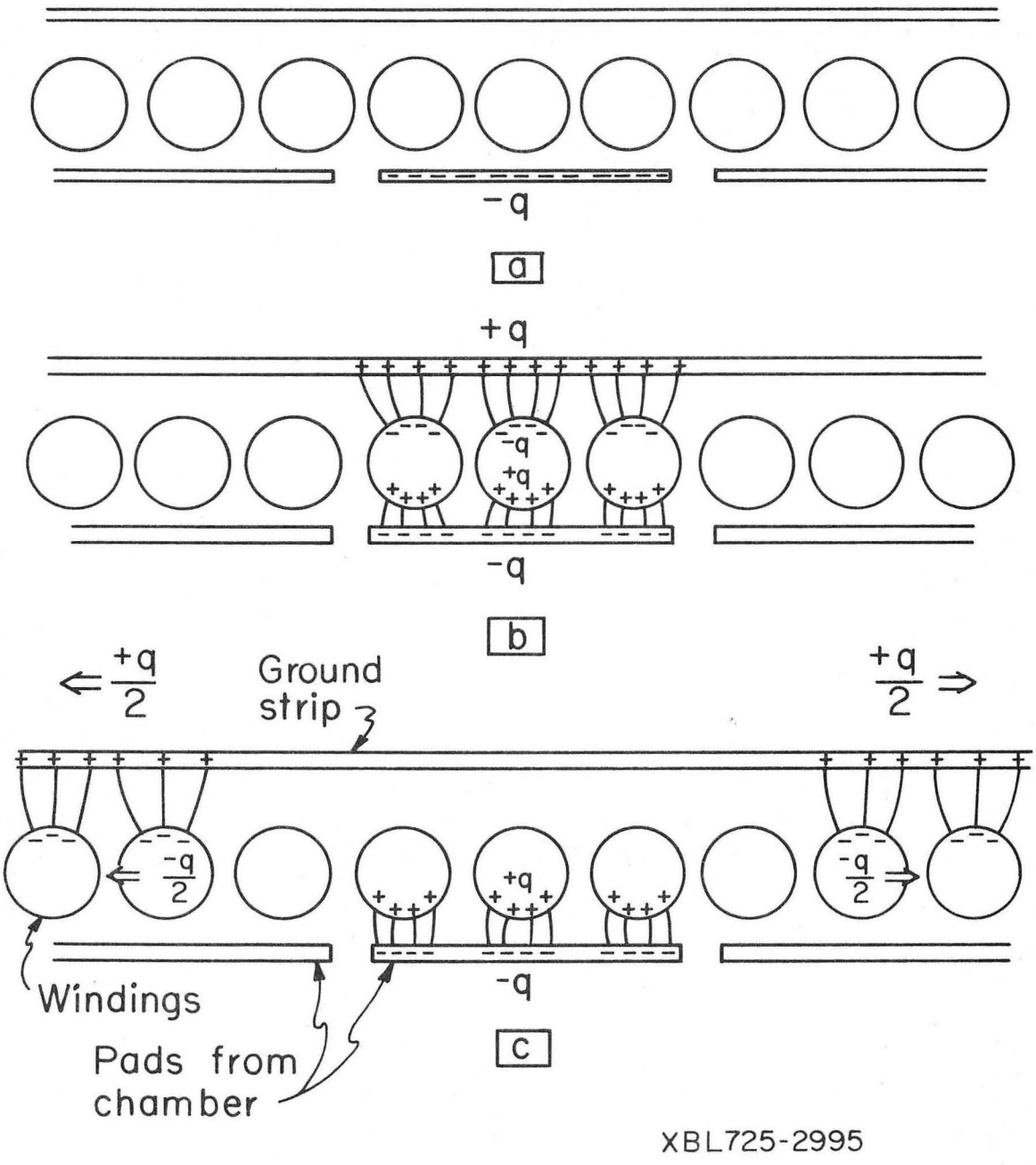

Fig. 21. Schematic cross section views of delay line and chamber pads. Charges that provide the DC chamber field are not shown.

voltage (which was 70% of the pad-ground voltage), except that, due to the spread in arrival time of the charge on the pad and to the dispersion of the wave itself, the charge spreads out over a distance d_{wave} ≡ full width at half height > d_{pad}, reducing the peak voltage. The resultant voltage ratio, $1/2 \times 0.70 \times d_{pad}/d_{wave}$, is in reasonable agreement with the measured value. Finally, long after the delay line signal has left, the charge on the pad leaks away through a resistor to ground.

Several sources of spurious pulses have been found and removed. On the Y = max side of the chamber, the Y and U_2 delay lines are adjacent, and signals jumped between them until we placed a shield (a sandwich of two sheets of bakelite and one of copper) between them. An interesting effect was seen when the U plane was <u>not</u> tied down with a delay line: a displaced pulse on the Y plane delay line whose position, relative to the main pulse, depended on the positiion of the source along the strip being read out (see Fig. 22). The induced pulse was bypassing part of the delay line by following the U strips. The jump from the U plane to the Y plane was made capacitatively.

Figure 23 shows a reflection caused by the edge of the copper plating and by the end of the delay line 5 cm further on. A, B, and C show the end reflection change as the terminating resistance is varied. The reflection at x is removed by inserting a grounded Cu strip halfway under the delay line. (When it is pushed under further, the reflection reappears.)

9. Prompt signal

Up to now we have gotten prompt signals from scintillators or from an unused plane (cathode or anode) from the proportional chamber. Neither will be possible with the muon identifier chambers, and getting a good prompt output without interfering the other three (X, Y, U) has proven to be nontrivial. Looking at the cathode common bus (Fig. 18) did not work well for reasons mentioned in section 8. A 2.5 cm wide Cu strip laid over the pads and separated from them by 50 μ of Mylar gave a good signal but degraded the rise time and peak amplitude

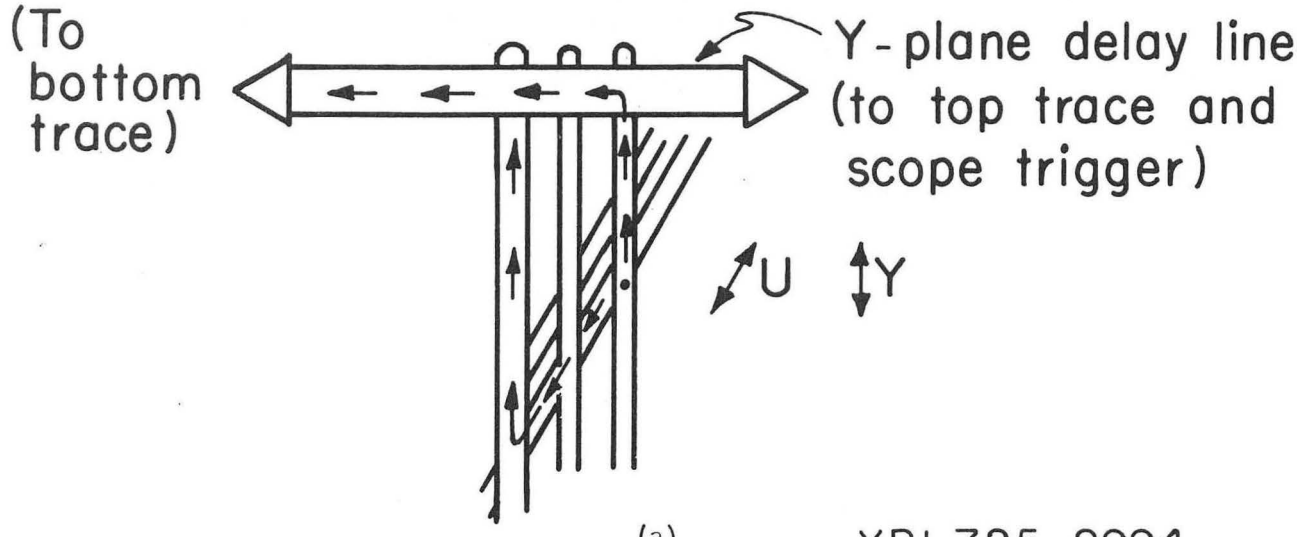

(a) XBL725-2994

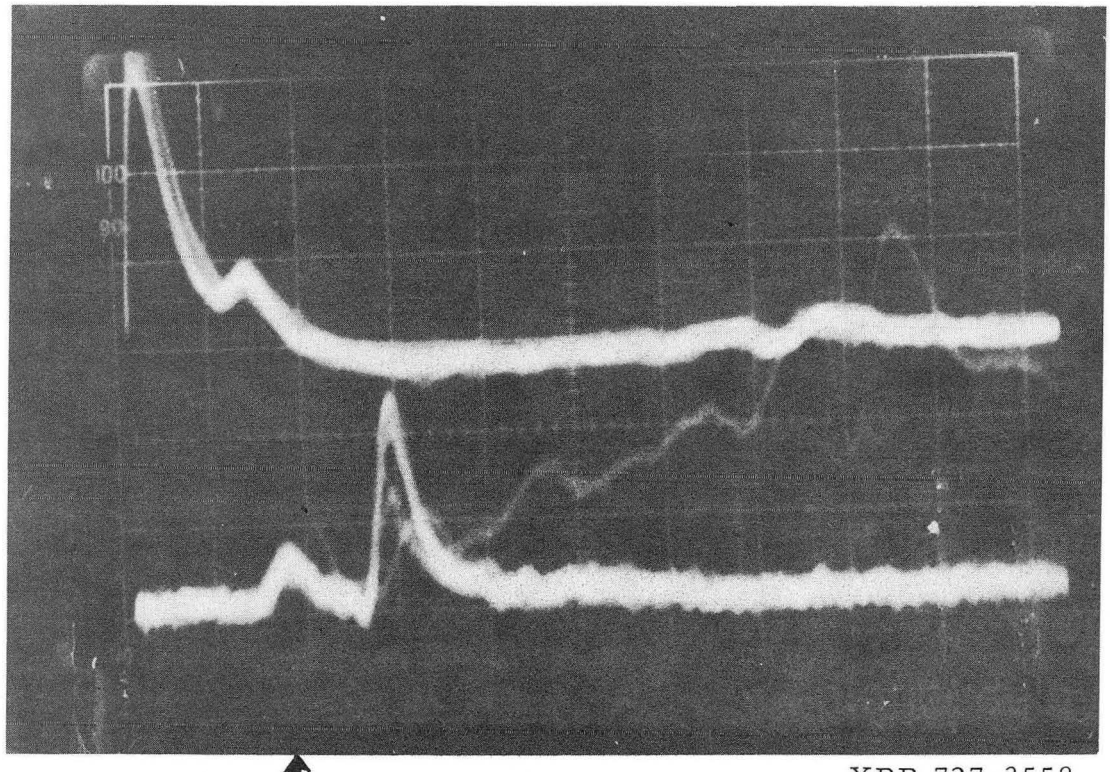

(b) XBB 727-3558

Fig. 22. Typical alternate induced signal path. (a) The path. (b) The signal. 2×4 mm gap, 20% CO_2 - 80% Ar, HV = 1.7 kV, 1 μsec/div. Top trace 0.1 V/div. Bottom trace 0.05 V/div. An arrow marks the displaced pulse.

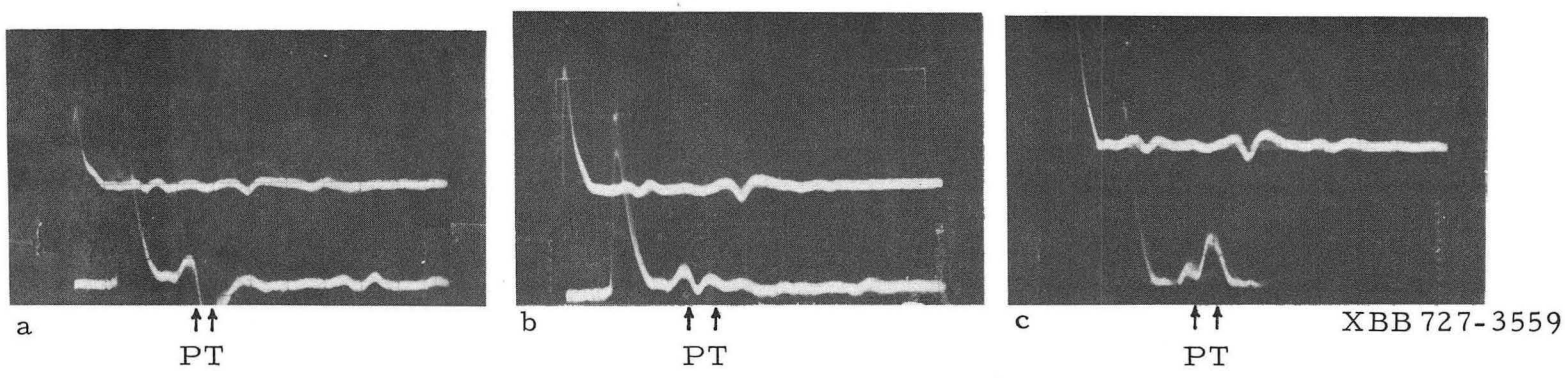

Fig. 23. Delay line reflections. 2×4 mm gap, 20% CO_2 - 80% Ar, HV = 1.7 kV, 0.2 V/div, 1 μsec/div. Anode plane delay line. Top trace: y = min end (triggers scope). Bottom trace: y = max end. Termination (a) small, (b) OK, (c) large. P marks the reflection due to the discontinuity in the plating, and T the one due to the terminating resistor.

of the delay line signal. The most promising method picks off a signal from the delay line ground.

Suppose the delay line ground strip is lifted from ground, as shown in Fig. 24, by resistor R_G. The ground strip current can now generate a prompt voltage signal. Both imputs to each delayed signal amplifier rise as the distributed capacitances are charged. (The inputs are tied together initially mainly by the winding-ground strip capacity.) Since the amplifier is a differential one, and has, in its output stage, a filter to block high frequencies, the prompt signal is suppressed. To complete the suppression it is necessary to add a common base input to the prompt amplifier to reduce its input impedance (to ~ 50 Ω) and hence the voltage swing of the delay line ground strip. The 0.01 μF low voltage capacitors shown prevent the DC bias currents of one amplifier from affecting the others. The diodes protect the Fairchild μA-733 IC's from large voltage swings, and the 200 pF capacitor reduces ringing. The 10 K's provide a DC return.

Full details of the delay line amplifiers are shown in Fig. 25. They were designed by Kai Lee, who also suggested using the ground strip pickoff.

Figure 26a shows the prompt and delayed outputs from the wire plane delay line. Attenuation along the delay line (new type) can be seen, comparing the y = 30, 23, 15, and 8 cm traces.

Initially the small ringing on the prompt output was far worse (see Fig. 26b). This turned out to be due to one of the two U plane delay lines being off at the time the tests were started. The source was nowhere near the affected section, but the signal took two capacitative jumps following paths such as the one shown in Fig. 27. As the delayed signal progressed down the structure composed of the delay line and the coupled Y plane strips, similar paths were created, causing the observed ringing.

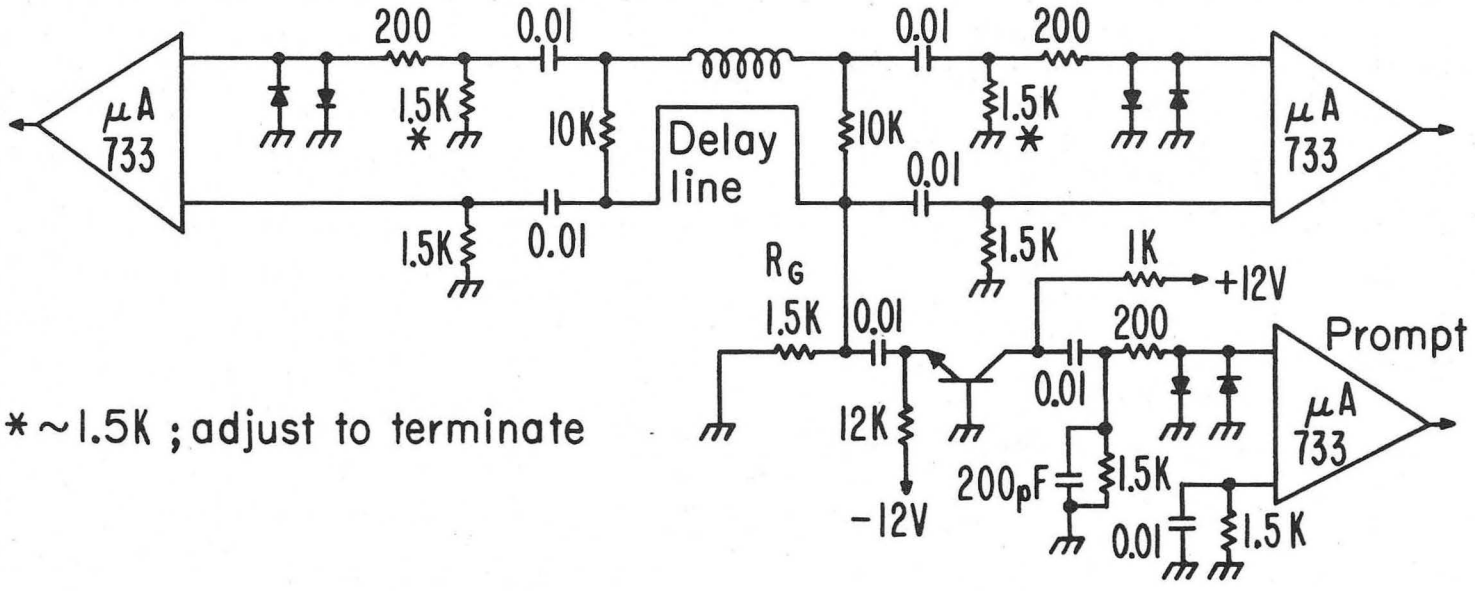

Fig. 24. Prompt output schematic.

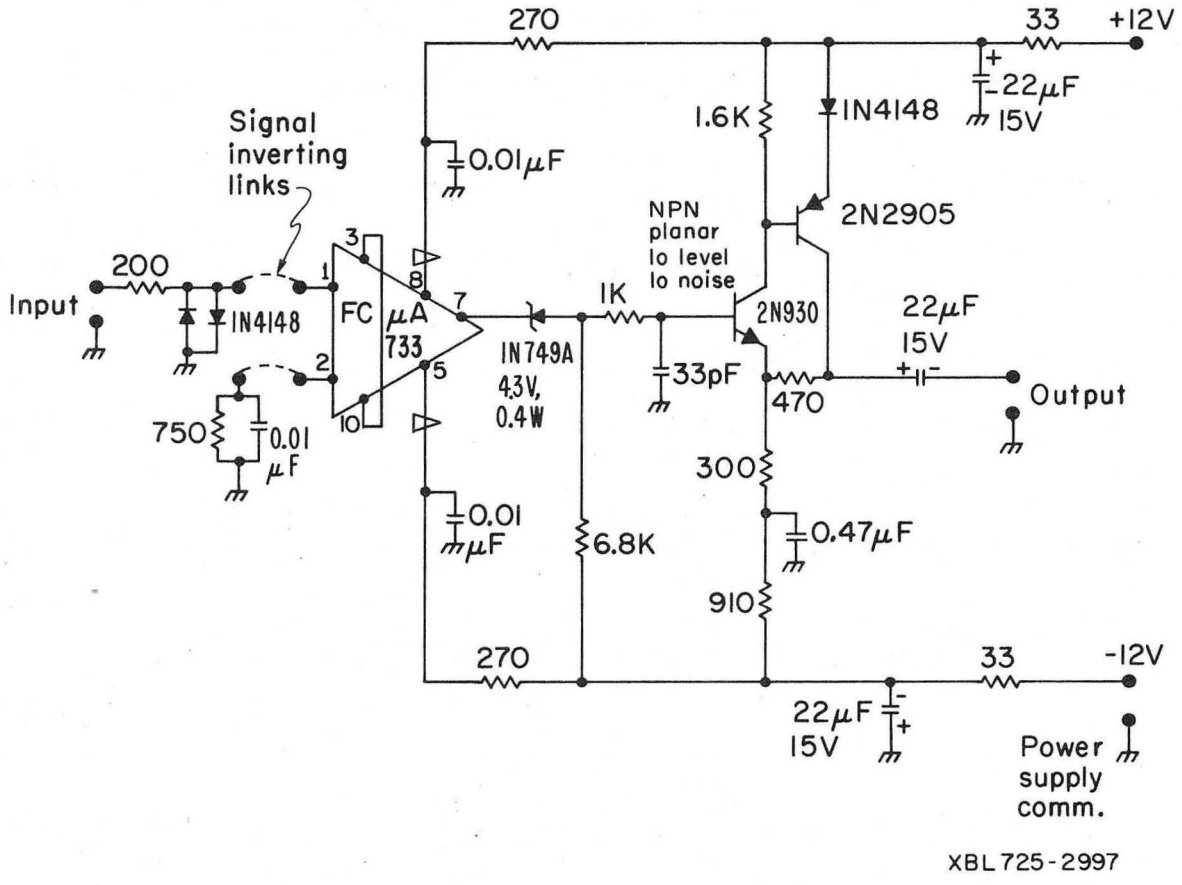

Fig. 25. Delay line amplifier schematic.

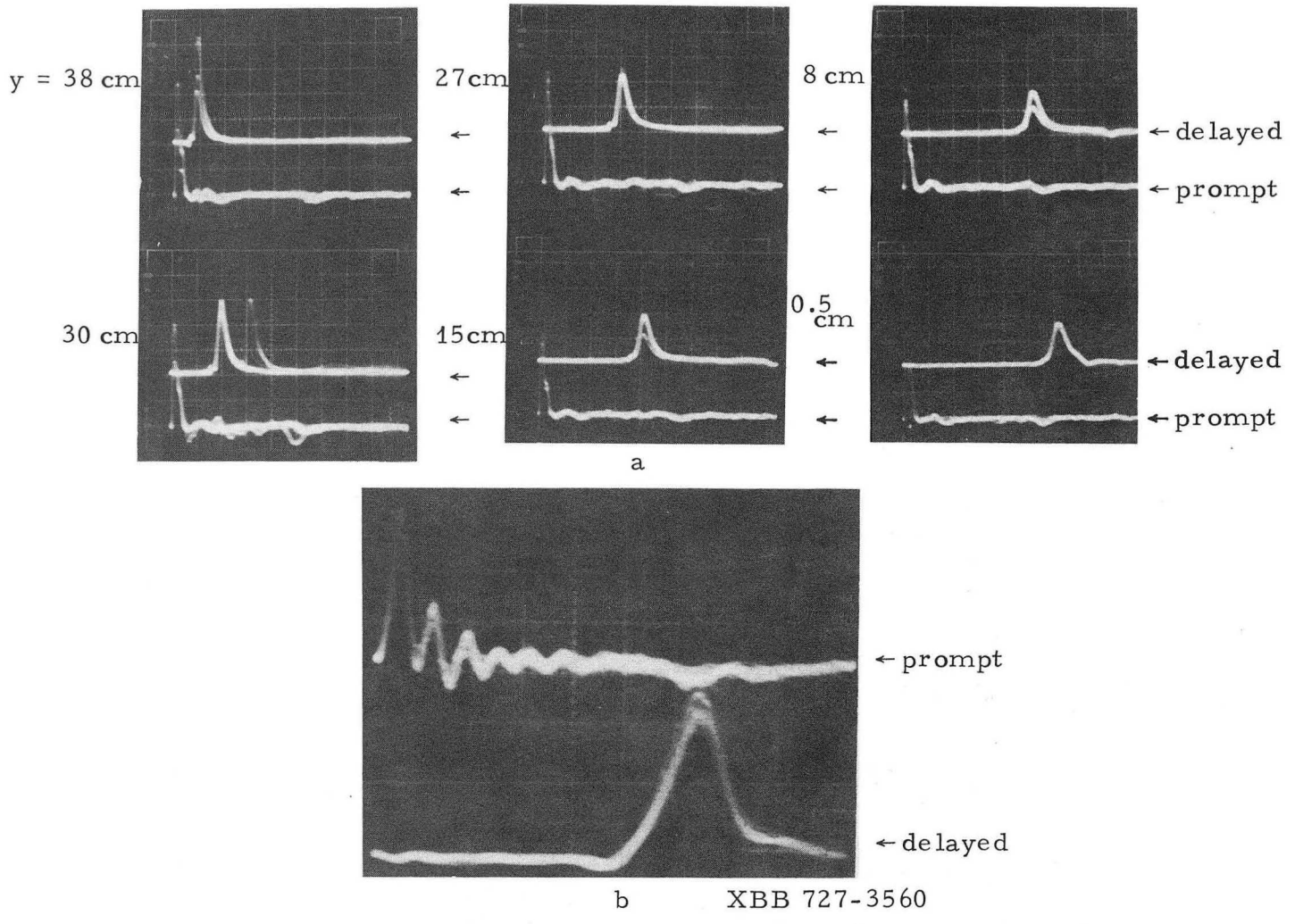

Fig. 26. Prompt and delayed amplified outputs from ^{55}Fe. 2×8 mm gap, 20% CO_2 - 80% Ar, 2.4 kV, 0.2 V/div, 0.5 μsec/div. (a) Normal operation, (b) ringing from U plane.

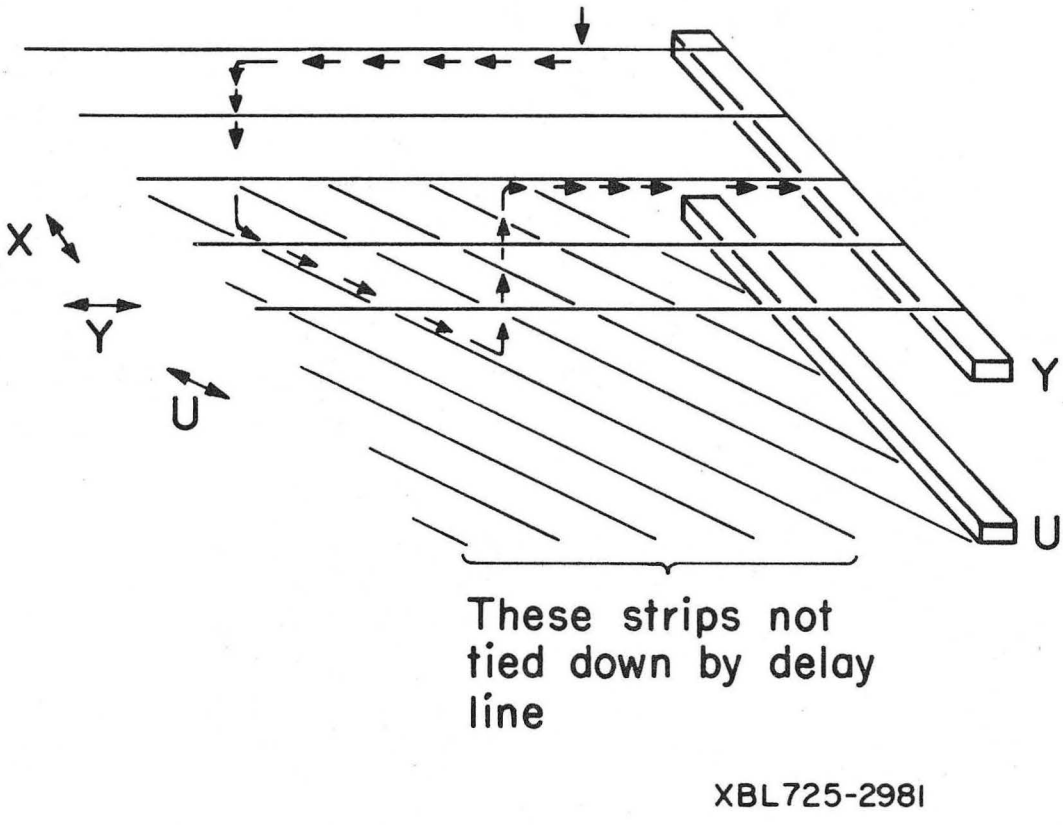

Fig. 27. Alternate signal path when cathode plane is not tied down by delay lines.

Figure 28 shows the signals before and after 120 m of RG 55U coax. The cost for this cable is 6¢ per foot. RG 58U which is similar (17.8 db/100 ft. at 10^9 Hz vs 16 db for RG 55U) costs 3.2¢ per foot.

10. Two track resolution

An estimate of two track resolution was made by connecting two of the chamber wires and putting a collimated ^{55}Fe source on one of them as shown in Fig. 29. Figure 30 shows the output of preamp A and (upper trace) discriminator with the source in positions 1 and 2. The two signals are of unequal height because the induced pulses of opposite sign on the adjacent wires go only to one of the two. The resolution distance increases by about 40 to 50% for preamp B which receives the signals through nearly the full length of the delay line. Overall, the two pulse resolution averages about 4 to 5 cm and ranges from 2.5 to 6.5 cm. Intermediate values are found when three wires are tied over to provide more nearly equal pulses.

11. Time resolution

The time resolution of the chamber was determined by triggering the scope on a scintillator signal from ^{90}Sr's with the set up described in section 5 and measuring the jitter of the prompt output. Figure 31 shows the prompt output (top trace) and the output of a zero-crossing discriminator (bottom 8 traces). Time slewing due to amplitude variation was about 10 nsec. The full width at half max is 50 nsec, and slightly more than 90% of the discriminator pulses come within ±50 nsec of the mean. The remaining 10% are all early. A more detailed study will be made of the time resolution when the computer readout is completed.

12. DC circuit

The DC circuit, shown in Fig. 32, is essentially the same as that for the 0.2 m chambers. The chamber has also been run with

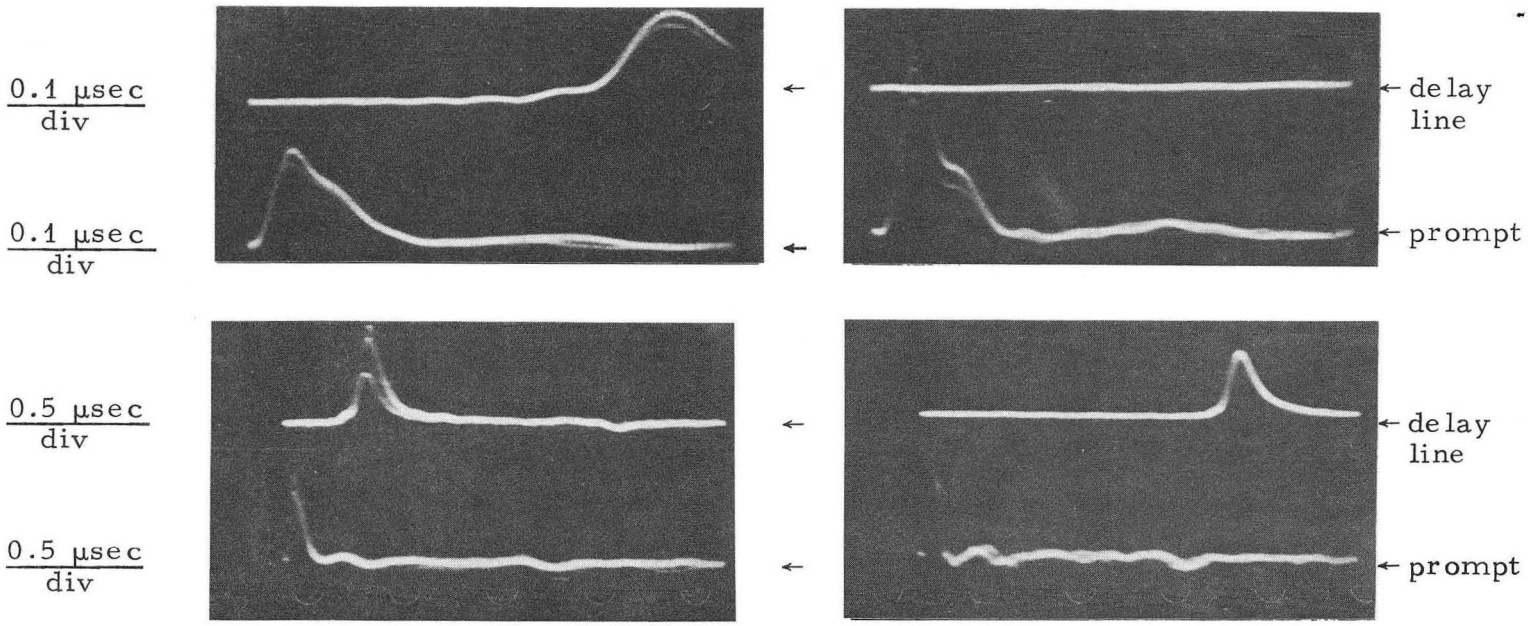

Fig. 28

Fig. 28. Effect of 120 m of coax cable on signals. 2×8 mm gap, 20% CO_2 - 80% Ar, 2.4 kV, 0.2 V/div.

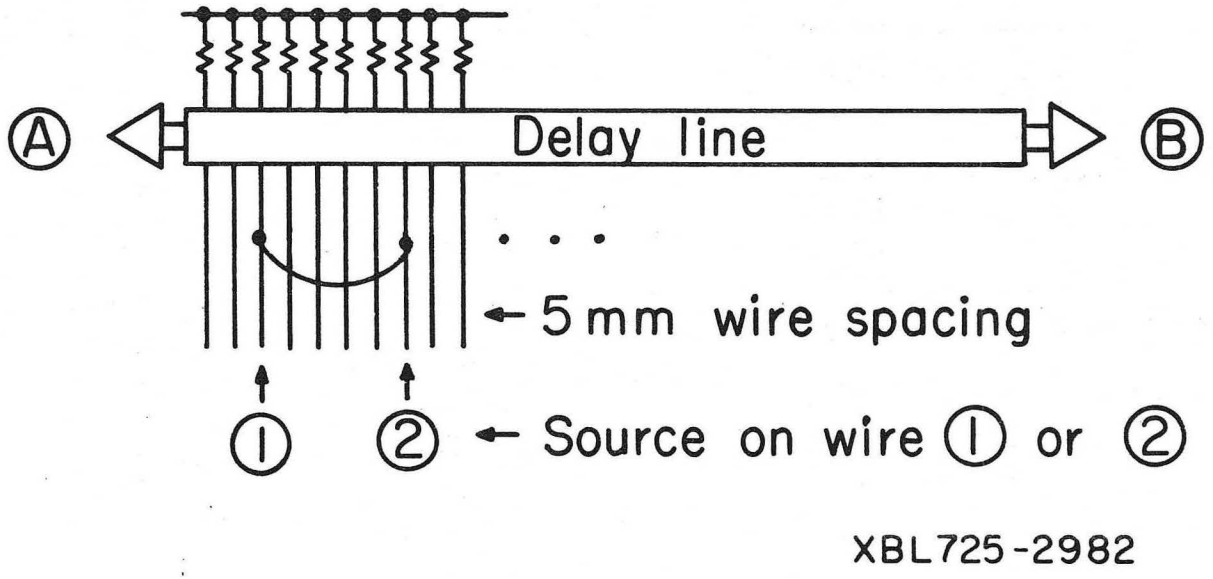

Fig. 29. Two track resolution test setup.

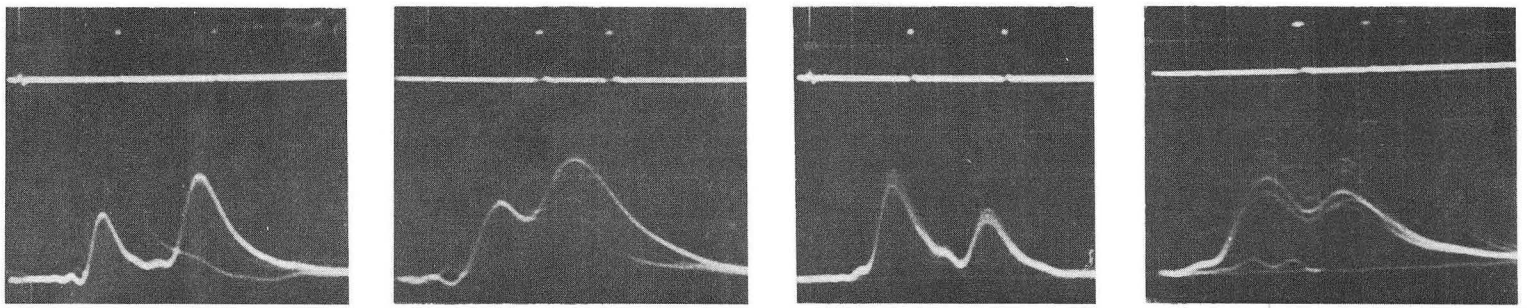

wire separation:	13	5	13	6
source position:	1	1	2	2
sweep speed :	200 nsec/div	100 nsec/div	200 nsec/div	100 nsec/div

XBB 727-3552

Fig. 30. Two track resolution. 2×8 mm gap, 20% CO_2 - 80% Ar, 2.4 kV. Top traces: discriminator output, 1 V/div. Bottom traces: preamp (end A) output, 0.2 V/div.

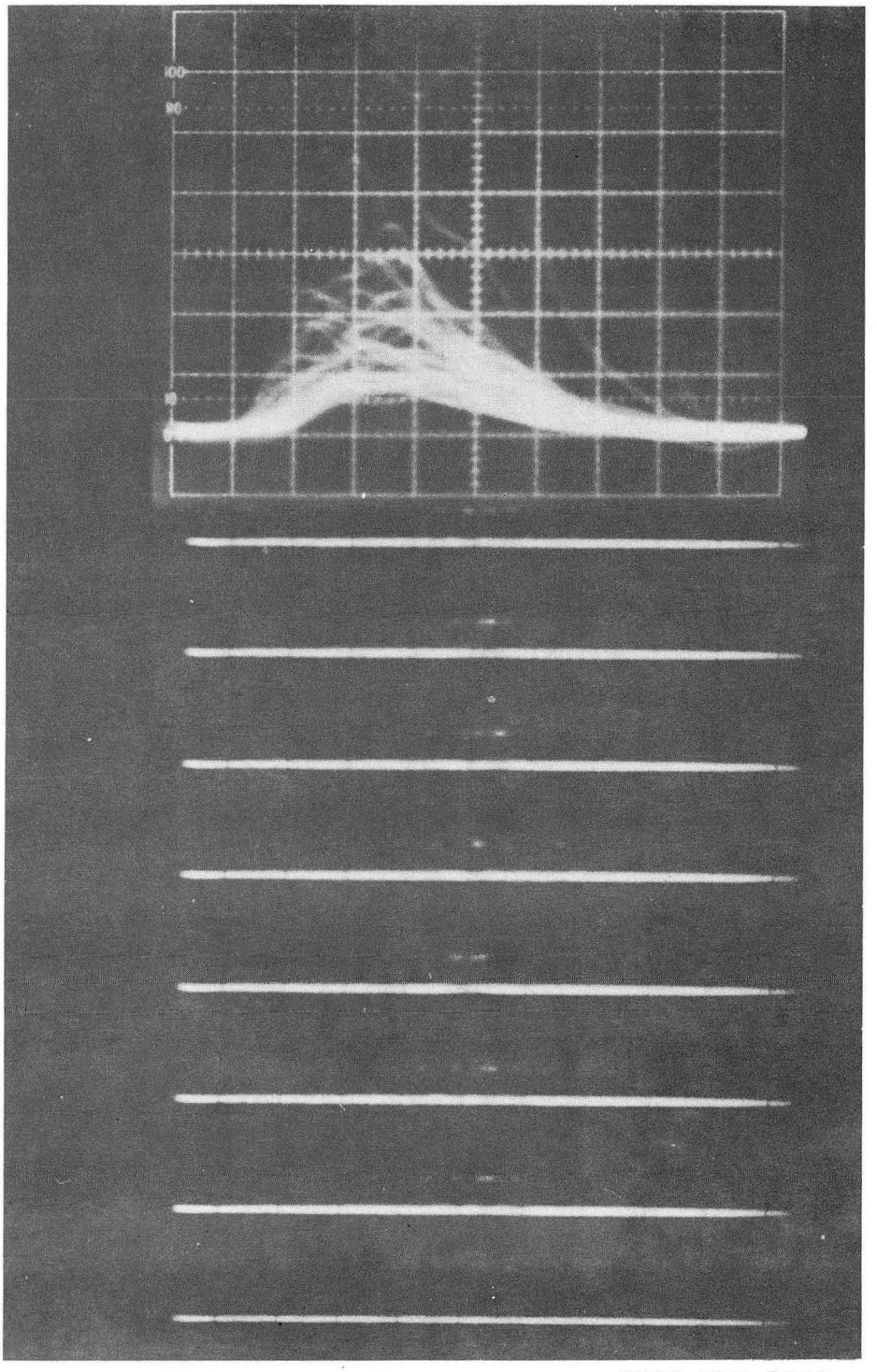

XBB 727-3553

Fig. 31. Time resolution. Top trace (35 sweeps)--prompt output from ^{90}Sr signal, (0.2V/div.). Bottom 8 traces (5 sweeps per trace)--zero-crossing discriminator output, 2V/div. 2×8 mm gap, 20% CO_2 - 80% Ar, 2.4 kV, 50 nsec/div.

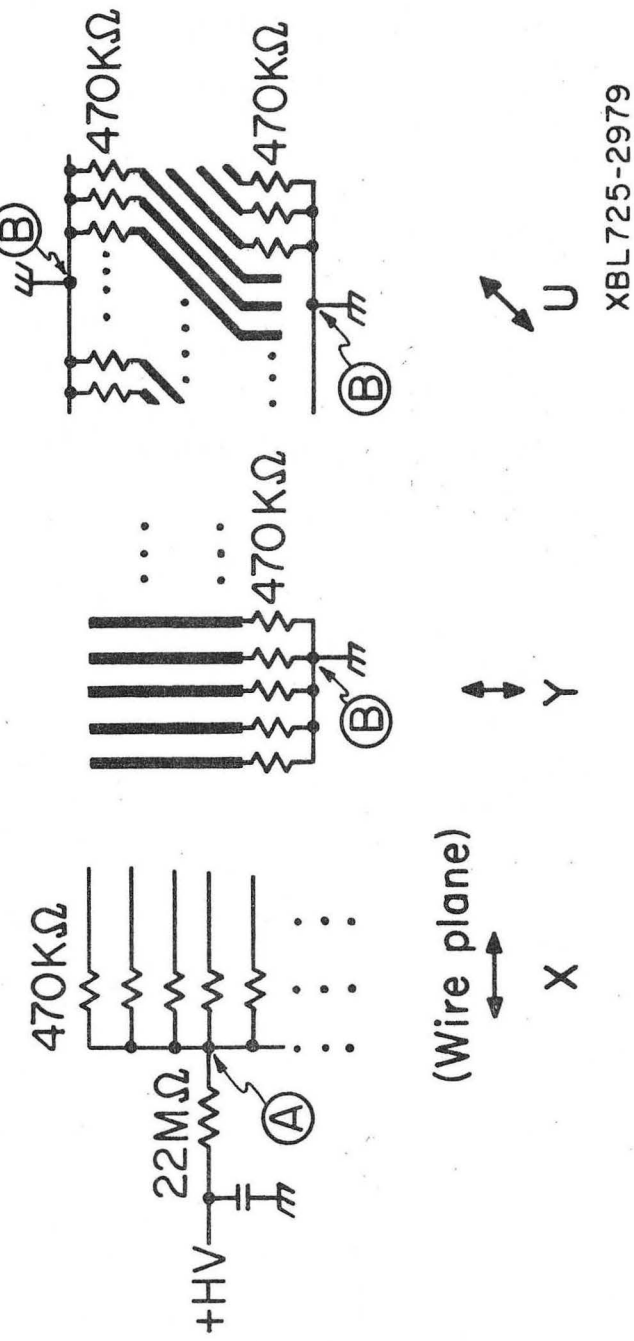

Fig. 32. DC circuit.

point A tied to ground and points B brought to negative high voltage through the 22 MΩ resistor to allow a direct measurement of the signal on the central wires with a 1:1 probe. No difference in chamber operation was seen (or expected). In the course of the testing, the chamber has survived several disasters (turning the 1000 V knob instead of the 100 V knob (SP), reversing polarity instead of changing voltage (RJ), ···) with no damage (except possibly to the experimenter's nerves). This is undoubtedly due to the 22 MΩ resistor which should be chained in, in all future installations. With chambers larger than the present one, the chamber capacity becomes large enough to store a damaging amount of energy (rule of thumb for 2 kV and 20 μ stainless steel wire: 10^2 pF is OK, 10^3 pF is marginal, 10^4 pF is too much). Then the 470 KΩ resistors will provide self isolation for the chamber as well as for the delay lines.

REFERENCES

1. R. Grove, I. Ko, B. Leskovar, and V. Perez-Mendez, Nucl. Instr. and Meth. 99, 381 (1972).
2. T. Trippe, Minimum Tension Requirement for Charpak Chamber Wires, CERN NP Internal Report 69-18 (1969).
3. Ray Fuzesy, Lawrence Berkeley Laboratory, (private communication).
4. Stainless 304, bright finish, as-drawn condition, from the California Fine Wire Co., P. O. Box 446, Grover City, Ca. 93433, was used. Rotomet flux, type SS from Rotometals, 980 Harrison St., San Francisco, Ca. was used in soldering.
5. S. Parker, R. Jones, J. Kadyk, M. L. Stevenson, T. Katsura, V. Z. Peterson, and D. Yount, Nucl. Instr. and Meth. 97, 181 (1971).
6. A. Morse and B. Feshbach, Methods of Theoretical Physics, McGraw-Hill, New York, 1953, p. 1236.
7. R. Muller, S. Derenzo, Lawrence Berkeley Laboratory, (private communication).

TECHNICAL INFORMATION DIVISION
LAWRENCE BERKELEY LABORATORY
UNIVERSITY OF CALIFORNIA
BERKELEY, CALIFORNIA 94720